TÉCNICO LISBOA

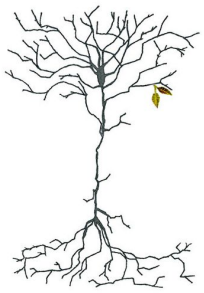

The spatial structure of surround modulation in mouse visual cortex

Beatriz Ferreira Belbut

Thesis to obtain the Master of Science Degree in

Physics Engineering

Supervisor(s): PhD Leopoldo Petreanu and Prof. Bruno Gonçalves

Examination Committee

Chairperson: Prof.
Supervisor: PhD Leopoldo Petreanu
Co-Supervisor: Prof. Bruno Gonçalves
Members of the Committe: Dr.
Prof. Lorem Ipsum

September 2018

We are so familiar with seeing, that it takes a leap of imagination to realize that there are problems to be solved. But consider it. We are given tiny distorted upside-down images in the eyes, and we see separate solid objects in surrounding space. From the patterns of stimulation on the retina we perceive the world of objects and this is nothing short of a miracle.

Acknowledgments

Leopoldo: Biology, hardware, previous software, guidance Tiago Marques: experiments and analysis Gabriela Fiorze: experiments Rhadika: surgeries Oihane: suit2p and surgeries

Rodrigo, Marina, Camille, Hedi discussions, input, environment

Alberto Vale discussion image treatment Bruno Gonçalves connection to Técnico's physics department?

All Champalimaud colleagues and staff: CISS, posters, talks, seminars, knowledge of neuroscience

Abstract

The Objective of this Work ... (English)

Keywords

Keywords (English)

Resumo

O objectivo

Palavras Chave

Palavras-Chave

Contents

List of Figures

List of Tables

Abbreviations

List of Symbols

1

Introduction

Contents

1.1 A systems neuroscience question: How does the nervous system perceive the visual world?

Neuroscience strives to understand the organization of the nervous system, it's function and processes, as well as its relation to animal behaviour. These broad goals require a multidisciplinary integration of concepts and tools derived from biology, biophysics, anatomy, genetics, statistics, modelling, computation, ecology and psychology. Furthermore,these questions can be approached at multiple scales: from the molecular and cellular levels to the systems and neural circuits levels.

Neurons and glia, the fundamental cells in a nervous system, agglomerate in neural circuits. In the human brain, there are about 10^11 neurons, of a great morphological and functional variety. Moreover, neurons are adaptive cells: each neurons can behave differently depending on the connections and signals it receives and transmits. Thus, disentangling the fundamental parameters of neuronal complexity and understanding the function of the nervous system require not only the signals and individual cell biophysical comprehension but also the understanding of the connectivity circuitry and mechanisms underlying a larger-scale neuronal network. Two systems with the same cells, arranged and interleaved with different connections would not behave equally. Correspondingly, the established knowledge on molecular and cellular neuroscience shall be integrated and complemented by a systems neuroscience approach, not as a simpler scaling step but within fundamentally different strategies. Investigating and deciphering the extraordinary questions about the nervous system in higher order completeness demand different methods, analysis and experimental paradigms than those within the study of the sum of its parts.

Neuronal systems can be described in three main functional sets: Sensory systems, motor systems and associational systems that link the former with the latter, developing more complex cognitive processes, such as perception, attention and emotions.

Animals have the enriching ability to sense the world around them. We sense our surroundings through efficiently designed stimuli sensors, and produce distinctive sensations accordingly. We are equipped with exceptionally sensible, accurate and complete input feature detectors.

However, perhaps one of the most fascinating qualities about a sensorial experience is that we can mentally encapsulate it as a given configuration and readily identify it at a future similar reoccurrence. Our nervous system allows the formation of a correspondence map between the world outside and the interior reality. The computational processing level and the efficiency of such endeavour continues to excite laborious research: How does perception arise?

In particular, the process of *seeing* pertains astoundingly substantial and relevant information about the world in a remarkably efficient, fast, detailed and engaging way.

The understanding of visual perception and its processes is undertaken as one of the major withstanding challenges in systems neuroscience.

In this case, the system receives the physical image information from the retina and then parallel processes the features from the current state of the visual scene in an hierarchically organized neuronal structure. The information signals follow feedforward pathways and integrations are then carried in

higher brain areas. Concurrently, feedback connections are superimposed in multiple higher order to lower order area connections, transmitting signals that underlie contextual information. Receiving this higher complexity input, neurons can then change their functioning state and produce new conjectures, educated guesses of high success probability about the input's nature. The unification of these parallel outputs is proposed to finally amount to a conscious sensorial perception.

There is no identity complete copy of the world outside within our perceived reality - Nonetheless, perhaps contrary to our intuition, sensitive sophisticated guesses can be just as effective, while efficient and biologically feasible within nature's parsimonious frames.

Nonetheless, fundamental questions remain for the large and complete understanding of sensory perception. In particular, discovering the computations held in the sensory cortices, their functionality, as well as the circuitry substrates that serve these mechanisms stand as main goals.

Here, we tackle a sensory neuronal property that is fundamentally implicated in visual information processing and that can yield profound insight onto the neuronal circuitry leading to visual perception - surround modulation (SM).

Neurons in the primary visual cortex (V1) respond to visual stimuli when it is presented in a given region of the visual field. For each visually responsive neuron, there is thus a *receptive field* (RF) - presenting a visual stimulus of optimal parameters to that neuron in the RF corresponding visual region, will evoke a spiking response. By definition, presenting stimuli outside the RF of a neuron will amount to no response in that cell. However, the simultaneous presentation of stimuli inside and outside the RF of a neuron will lead to a modulation of the cell's signal: the response will be either suppressed or facilitated in regards to the RF-only condition, depending on the center and surround stimuli characteristics.

This property is always active during vision processes, has been described in several species (mouse, cat, primates, humans), in various visual system areas (from the retina to the extrastriate cortex) and in multiple sensory modalities (visual, auditory, somatosensory, olfactory). A mechanistic SM theory would in this way provide a manifestly important framework in which to understand sensory processing. Moreover, understanding the circuitry that results in the SM effect and accounts for its properties can lead to insight about the function and the organization of the involved connections and network patterns - in particular, SM characterization can aid restrain circuitry models and interpret the network of inhibitory and excitatory neurons as well as feedforward, feedback and horizontal connections functionality in that perceptual integration context.

Most specifically, *far* surround modulation has been suggested to require feedback input.

Typically, SM is studied in either of two methods: By using radius expanding circular grating patches or by using grating patches confined to the RF area and surrounded with annular gratings whose inner radius are made to decrease. These studies have lead to important findings about the properties of SM and elicited fruitful debate on the circuitry architectures that can result in these characteristics in a compatible way.

However, these approaches focus on static stimuli and further assume the effect's isotropy and circular symmetry.

Recent work in mice has revealed that feedback connections from MT to V1 do not target lower-order areas irrespectively of the tuning of the higher-order sending areas. This study portrays that feedback mainly targets lower-order neurons that respond to the same positions in the visual field as the former, but that a subset of these connections are in fact dispersed to other neurons: If a higher-order neuron is tuned to a particular direction, it presents a bias to connect to a lower-order neuron that responds to the visual field positions that would appear *before* in that direction line. Similarly, if a high-order neuron is orientation tuned, it presents a bias for connecting to lower-order neurons that map visual field regions at orthogonal zones to that high-order neuron's preferred orientation.

Given the putative relation between feedback and SM, this suggested possible anisotropies in the SM effect itself, possibly to relate and to put at the perspective of the viable circuitry involved.

Here, we present an extensive characterization of SM in transgenic mice's primary visual cortex performed with two photon imaging techniques that allowed access to large datasets of differently tuned neuronal responses. We developed a moving grating stimuli presentation protocol of multiple combinations of movement directions and spatial locations that enabled the study of the spatial structure of SM and its nonuniformity.

1.2 State of The Art

State of The Art Section.

1.2.1 Dummy Subsection A

State of Art Subsection A

1.2.2 Dummy Subsection B

State of Art Subsection B

1.3 Original Contributions

Contributions Section.

1.4 Thesis Outline

Outline Section.

2

Theoretical Introduction

Contents

Present the chapter content.

2.1 Visual Neuroscience: Perception

2.2 Brain visual pathways

2.2.1 The eye

Most of the visual relevant information we receive consists of spatial and time variations in light intensity. When receiving light, the retina maps the light's temporal and spatial patterns onto a layer of receptor cells that respond to light with an electrical activity pattern in a retinotopical map: organized, topographically ordered representations of the visual field.

The retina is the innermost layer of the eye, and a part of the central nervous system. It contains light-sensitive neurons, photoreceptors, and allows for the transmission of visual signals through another class of neurons, the ganglion cells. It also contains horizontal, bipolar and amacrine cells. Horizontal and amacrine cells mediate lateral interactions. The major route of information in the retina follows from the photoreceptors to the bipolar cells and finally to the ganglion cells. Each ganglion cell responds by changing its firing rate to stimulation of a roughly circular concentric patch of the retina, its classical *receptive field* [**?**]. This information is then relayed to the brain.

The photoreceptors, rods and cons, are the first intervenients, and account respectively to the sensitivity and the acuity in the detection of light. When light falls in the retina's photoreceptors, they are activated by means of grated changes in membrane potentials that then induce corresponding changes in the rate of synaptic transmitter release from ganglion cells.

To allow the eye to respond efficiently over great spatial and temporal ranges in illumination intensity, this regulation's criteria is based on judicious input's pattern transformations. Both the temporal and spatial conversions code information by means of giving prominence to rapid *changes* and filtering out slow changes in light intensity over time and space.

Concerning the spatial pattern, the question becomes, how are the different receptors responses jointly treated? In fact, *lateral inhibition* arises: If, while in the dark, a small light stimulus appears, rod cell's will be enhanced. The rod cells corresponding to the center of the stimulus' location will send an activated signal. However, due to lateral inhibition from horizontal cells, the different rod cells outside the stimulus' location will send an inhibitory signal. This implies the prominence of boundaries between bright and dimmed regions.

The sensitivity to light-dark borders in the visual scene is further achieved by the two ganglion cells classes, on-center and off-center. These cells are sensitive to differences between illumination levels in its receptive field center and in its ring-shaped surround. In an on-center ganglion cell, brightly illuminating a central spot of the receptive field produces a burst of action potentials. In an off-center cell, the response to the same stimulus is a reduced rate of action potentials, and an increase as the illumination is turned off.

2.2.2 Central Visual Pathways

Firstly, the primary visual pathway mediates vision and visual perception. Information is driven from the retina, to the thalamic dorsal lateral geniculate nucleus (LGN) and finally to the primary visual cortex (V1).

Ganglion cell's axons follow a path over the retina's surface to the optic disk, bundling together in the optic nerve. From here, the ganglionic axons continue to the optic chiasm, past which the axons from both sides form the optic tract. These axons then continue to the brain, mainly projecting in the dorsal lateral geniculate nucleous (LGN) in the thalamus. The LGN is arranged in layers and appears in both brain hemispheres, receiving information from the left and right semifields of view detected by each of the two retinas. These then radiate to the striate cortex, in the primary visual cortex V1, mostly to layer 4 (out of 6 functionally distinct ones).

In both LGN and V1, the retinotopy in mantained. In accounts for these cells stimulus response organization, the LGN cell's receptive fields are concentric and ruled analogously to those from the ganglion cells. However, the striate cortex's V1 cells can have different organizations of their receptive fields, with different distributions and numbers of excitatory and inhibitory areas.

Furthermore, neurons in the striate cortex have an added property: they can be tuned, and present selectivity to particular features. A neuron's tuning can be specified for any stimuli space, and its responsiveness measured for different points within that space.

Foremost, the response of neurons in cortical areas such as V1 is found to be tuned to orientation of edges. The orientation to which a given cell produces the larger response is called the preferred orientation of the neuron, and all orientations are equally represented in the visual cortex. V1 neurons are mostly organized in columns of different selectivity to particular stimuli attributes: Across layers, in the same direction, neurons respond to the same orientation. Hence, receptive fields are repeatedly represented into modular sheets of neuron distributions in each sublayer. Furthermore, some cortical neurons are selective to lengths or to the direction of stimuli bars, to color, spatial frequency or ocular preference - relative strength of the input from the two eyes.

Following from V1, extrastriate cortical areas are organized into two large systems: The ventral stream, following V1 to V2 to V4 and connecting to the the temporal lobe, thought to account for object recognition, high-resolution images treatment; and the dorsal stream, with a path from V1 to V2 to MT and connecting to the parietal lobe, thought to process the analysis of motion and positional relations between objects in a visual image, as well as attention control. Accordingly, neurons in the ventral stream are selectively tuned to shape, color, texture and, in higher levels, to faces and objects. It is however important to note that, for example, a given specific face's recognition is encoded by a specific pattern of activity in a population of cells, and not by the unique firing of a super-narrowly specific cell. On the other side, dorsal stream's neurons are selective to elements such as movement's direction and speed, containing a detailed map of the visual field.

Neurons at higher levels in the visual pathway are increasingly tuned, latent, and in general have larger receptive fields.

Ascending away from the striate cortex, an hierarchy can be recognized, evolving from the analysis

of simple attributes of an image, such as contrast, colour, orientation of segments, going to intermediate level vision, regarding contour integration and surface segmentation, and finally turning to more complex visual processings such as object recognition.

2.2.3 Feedforward: spatial filtering of natural images

Ganglion cells can be treated as low-pass spatial filters, producing responses to sinusoidal gratings having a variety of spatial frequencies, with a given range (the neuron's bandwidth) determined by the receptive field's size.

The neuron's bandwidth becomes narrower as we go from ganglion to LGN and then to striate cortex cells.

Particularly, simple cells can, in this sense, be described as Gabor functions [**?**], a product of a sine function and a gaussian envelope. This description accounts for the necessary trade-off in spatial frequency and spatial location specificity: A wider gaussian relates to a wider receptive field and thus a narrower spatial frequency bandwidth, but a larger set of possible stimulating spatial locations. This motivates the idea for the efficient encoding strategy of the natural visual world. In a given image, redundancy is expected: it is probable that the light reaching one photoreceptor will be strongly correlated to the light that reaches its neighbours, and thus, at first levels such as V1, high specificity is not required, and patterns can be more economically encoded.

On the other hand, striate cells can be regarded as bandpass filters, with a greater variation in the allowed spatial frequency tuning. The striate cortex processes many differently located patches from the retinal image, each containing different spatial frequencies, with the firing rate of each cell accounting for the amplitude of the frequency component to which the cell is tuned - a patch-wise Fourier analysis of the input image.

2.2.4 Feedback pathways and influences

Up until this point, this description has focused on the classical model of feedforward transmission of sensory information in an hierarchy of cortical visual areas, beginning with V1 and following through the ventral and the dorsal pathways. However, visual pathways are bidirectional. Superimposed in these bottom-up connections, there are reentrant pathways that transmit influences in the reversed top-down direction, in every stage of the visual pathways except for the retina.

To understand these reciprocal interacting mechanisms that can cause non-linear effects, another point must be made explicit: Neurons do not function as fixed functional processors, but rather as adaptive units that can change their function depending on the behavioral context, subject to attention, expectation and perceptual task instructions, at any given processing moment.

This adaptation appears via both changing of neurons' tunings to stimuli - changing of their receptive fields characteristics - and by alteration of the correlations structure of neuronal ensembles.

The neuron changes its *line label*, in accordance to higher orders instructions: A neuron's response means that a stimulus with its preferred attributes is being detected, being the signal as strong as the stimulus is close to that preferred configuration. However, accounting for feedback, a cell can function in different functional states and the meaning of the information they convey depends on that state -

its preferences are changed. The analysis is not misinterpreted because the higher areas that send the adaptative instruction to a given neuron or population of neurons also treat the resulting returning signal.

On the other hand, a network of neurons within the same, as well as across different cortical areas, can change their spatial and temporal distribution of correlated activity. In fact, if neurons can be made independent to one another, an ensemble of such neurons will have less variability than that of a single neuron's response to a given stimulus, allowing for better signal to noise ratios of that process and thus for more optimal information encoding.

Vision is then seen as an active process, with feedback conveying signals that adapt the lower neurons in such a way that allows them to encode more relevant information within a given contextual paradigm, facilitating the visual scene representation and interpretation: Their responses to a stimulus are made more informative about the identity of that stimulus. Moreover, given the complexity of the neural pathways, this idea implies that any given cell receives input, directly or indirectly, through feedforward or feedback entrances, from each other relevant processing stage, in a way representing the full brain on their own.

Beyond a straightforward low-level analysis of simple local attributes, under feedback influences, neurons can integrate six main different forms of contextual information: Spatial, object and feature oriented attention; the at hand perceptual task; object expectation; another behavioural context effect is the case of eye movement across a visual scene. For the image to continue appearing stable, an efference copy of the motor instruction for the eye movement is kept in higher cortical levels and this information is then sent to the retina that compensates for that signal; Finally, top-down influences can also provide memorized and learned information.

2.2.5 Surround modulation in the visual cortex

Thought to determine optimal coding efficiency, sensory processing and perception, neurons exhibit the surround modulation phenomenon:

A stimulus inside a neuron's RF will produce a response of activation in a small part of the visual field. While the same stimulus will not activate the neuron if it is represented outside its RF, if jointly presented in both regions, a modulation of the neuron's signal will take place. This facilitatory or inhibitory modulation will depend on the relative stimuli characteristics in both locations.

SM occurs in many species, sensorial systems and processing levels, including from the retina to neurons in the extrastriate cortex.

Summarily, SM in V1 accounts for five main attributes: It is spatially extensive, contrast dependent, develops rapidly in time and its properties are different across cortical layers. Most importantly, it is tuned to specific stimulus parameters, suppressing responses for stimuli in the RF and surround with the same orientation, spatial frequency, drift direction and speed and enhancing the signals for orthogonal parameters.

SM can evoke visual saliency, perception of boundaries, and figure-ground segregation. Furthermore, SM functional role could also be to reduce redundancies in neuronal responses and increase

response sparseness, making the full neuronal system more efficient. For instance, the finding that similarly oriented lines in the RF and the surround produce a suppressed signal can be intuited in the light that neighbour lines with the same inclination are statistically expected in a natural image and don't require a prominent encoding.

A working hypothesis [**?**] entails that SM can come from feedback, feedforward and horizontal connections, both with increased inhibition and reduced recurrent excitation of signals.

Nevertheless, great debate is still conducted on the mechanisms that can cause SM, as well as on the circuits that mediate it. Furthermore, the functional roles of feedback are yet to be fully described.

2.3 Surround modulation remaining questions and project's plan

In a cell, SM might not be isotropic and furthermore, its anisotropy may depend on the stimulus' nature, in general or relative to the regarded neuron's selectivity. However, most previous experiments on SM have been devised with circular stimuli varying in radius, assuming the effect's isotropy. The present project proposes to tackle the possible anisotropy itself.

Furthermore, so far, studies have mostly regarded individual neuron's SM properties in cat or monkey subjects. In mice, neurons with the same orientation selectivity do not lie in the same column. Neurons with different tunings are mixed. Since this thesis task will be conducted in mice, we can thus regard multiple neurons with different tunings at once, in a more complete approach.

A recent procedure has also been done with differently localized patches of gratings in the surround [**?**]. However, this was conducted with static stimuli, and was furthermore executed with limited stimuli configurations. Besides using moving gratings, this project's aim is to produce an extensive study on a multitude of neurons, tunings, and stimuli configurations: Only in this way can we pursue the finding of a set of more generalized and integral SM spatial structure rules.

Having these objectives in mind, experimental and analytical steps will comprise, for each mouse:

1. Imaging large populations of neurons (¿1000).

2. Measuring the neurons' receptive fields. These will be different from cell to cell.

3. Suiting the larger possible number of neurons, appropriate stimulus RF and surround sizes will be fixed. Only the neurons whose receptive field does not intersect the stimuli surround will be analyzed.

4. A central stimulus will be presented. This stimulus will be a moving grating that can have 4 different cardinal directions, thus exciting different neurons, according to their selectivities. First recordings will be for only this center stimuli (4 possibilities).

5. For each of these RF's stimuli displays, small patches of moving gratings will be simultaneously presented in the surround, under a variety of configurations:

Only one patch, that can be presented in 4 angular positions of the ring-shaped surround (N, E, S, W). For each of these locations, surround gratings' will have the two directions and 2 orthogonal orientations (64 possibilities).

Two patches located around the surround. These can be located in a vertical or horizontal direction line. For each of these configurations, the patches grating can further be with the same orientation or with opposite directions - no other relative orientation will be presented (16 possibilities).

6. Control recordings will also be operated only with surround gratings, to ensure that these are not directly driving the neuron and are by definition displayed in the surround (16 possibilities).

7. The large population of neurons' responses will then be analyzed, for each of these 100 possible configurations. Comparison across neurons and across configurations will then take place, as to produce a set of SM spatial structure rules and discover possible diversity and asymmetries in neurons' responses to stimuli.

2.4 Receptive fields and tuning

2.5 Feedback as a path for contextual information integration

2.6 Surround modulation

2.6.1 Suppression and facilitation

2.6.2 Spatial structure of the phenomenon

2.6.3 The motivation: feedback organization rules - uncovering the functions of feedback

Understanding feedback mechanisms and organization is an important step in advancing the comprehension of the numerous functions it has been implicated with [REFERENCES][**?**]: attention, awareness, working and associative memory, perceptual task, object expectation, prediction, scene segmentation, efference copy, perceptual learning. Furthermore, their role in cortical computation remains to be explained, in particular within the frame of theories of hierarchical cortical computation.

In recent work [**?**] the aim was to bring about organization rules that can constrain and suggest theories of feedback function. The problem approached was the organizational logic of feedback axons relaying inputs from the lateromedial visual area (LM) to the lower area V1 in mice. LM is one of the main sources of feedback input into V1 and is also a retinotopically organized map of the visual field.

For this, RFs in LM-feedback boutons into V1 were mapped and related to those of neurons in their V1 vicinity.

Firstly, in layers L1 and L5/6 - layers to which feedback information is diffusely relayed to, in the target area V1, with diverse feedback signals [**?**] - LM visual area inputs targeted, on average, retinotopically matched locations in V1, meaning that the connections were, on the average effect, from neurons that map RFs close to those RFs that the target neurons represented.

Despite this average organization, there was a high scattering of LM inputs in V1, with a large number of the considered LM feedback axons relaying visual information from distant points in the visual space. Thus, in a given location in V1, neurons have access to information from a wide area of the visual space from LM feedback inputs, with in fact a significant proportion of inputs with deviations larger than 30º.

Then the question turned to assessing if these deviations depended on the tuning properties of the LM boutons. The idea is that, in accounts to direction selective neurons, tuning-dependent wiring biases could relay predictive feedback signals of moving stimuli - image 2.1.

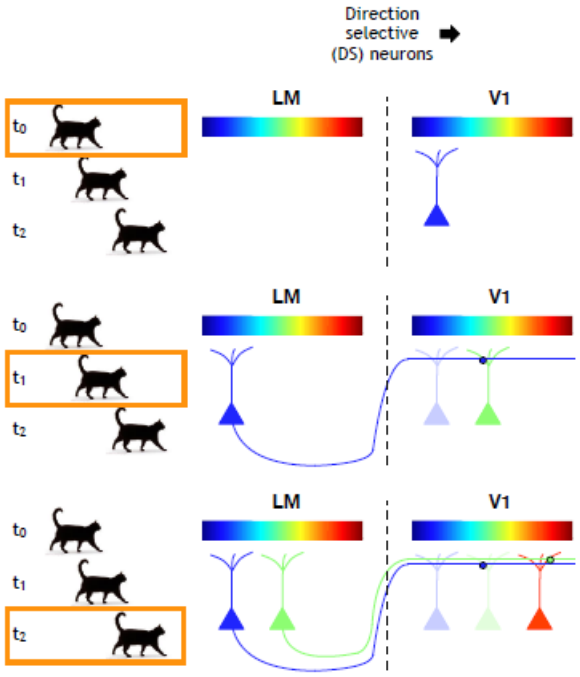

Figure 2.1: Feedback signals from LM to V1 could convey predictive information about a moving object, if we consider that their wiring is biased according to their own tuning. In this example, we consider direction selectivity tuning as the criteria for the feedback wiring.
Top: A stimulus (the cat) moving in a given direction (left to right) will activate neurons in V1 with that direction selectivity and with their receptive fields located at the corresponding region where the stimulus is in the subject's visual field at that time t_0 (left-side, blue labeled azimuth angle).
Middle: These DS left field-of-view corresponding neurons feedforward to neurons whose RF represents the same left-side location in the visual field. These would project back into V1 neurons corresponding to positions on the middle region (green-labeled azimuth angle) activated by the stimulus at t_1.
Down: These neurons, activated by the stimuli presentation in that visual field region, also connect retinotopically to LM cells with the same direction selectivity. Again, these project to the neurons corresponding to the RF position ahead (right-side, red-labeled azimuth angle), activated by the stimulus at t_2).
In this way, predictions on the next cat's position, as assumed by the direction it followed at previous times, could be relayed via feedback from LM to V1 neurons.

Image from the presentation by one of the principal co-authors of [?], Tiago Marques, under the Champalimaud Internal Seminar Series on October 15^{th} 2017, *The functional organization of cortical feedback.*

Different orientation selective neurons are intermingled in L1 of V1. This allows the simultaneous analysis and comparison of the effects of various tuning properties.

The experimental results showed that the retinotopic deviations depend on the feedback orientation and direction selectivities, according to simple geometrical rules - figure 2.2.

Orientation-selective (OS) LM axons overspread around the retinotopically matched location in V1 perpendicularly to their preferred orientation. Moreover, analysis on direction-selective (DS) axons

presented that these overspread to areas shifted from the retinotopically matched position along the angle of their antipreferred direction. EXPLAIN BETTER. CHECK WORDING.

In this way, LM feedback axons could enhance visual representations in space and time, by targeting cells in V1 that would be activated by stimuli perpendicular to or opposite to their own tuning. EXPLAIN AND CONCLUDE BETTER.

ADICIONAR REFERÊNCIAS NECESSÁRIAS

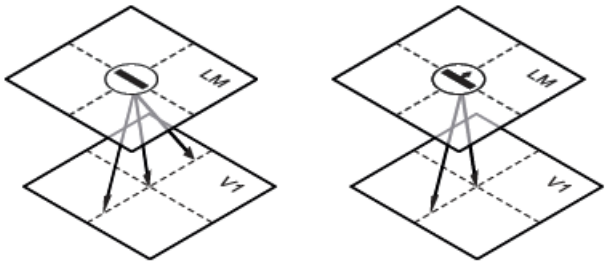

Figure 2.2: LM feedback to V1 functional organization acording to simple geometrical rules. Planes represent retinotopic maps in V1 and LM, while bars represent preferred orientation of the LM neurons.
Left: OS inputs have biased wiring towards positions ortogonal to their preferred orientation.
Right: DS inputs tend to be wired along the opposite sense to their preferred motion direction. CHECK THIS WORDING

Images from [**?**].

3

Technology

Contents

Developing precise and reliable tools for the spatial and temporal mapping of neuronal activity is crucial to understand the functional architecture of the brain. Radiotracer, electrophisiological, magnetic resonance, anatomic and optical imaging techniques all offer advantages and disadvantages to this end [REFERENCES]. On its part, optical imaging of neuronal activity allows the mapping of large regions of the cortex, varying in time as responses to stimuli. This can be acomplished with voltage sensitive dyes [REFERENCES], changes in the optical properties of the tissue or with the aid of genetic tools. In here, we review the utilized techniques: Intrinsic optical signal imaging that draws on the changing reflectance in the hemodynamics of the cortex and two-photon laser microscopy that takes advantage of genetic manipulation tools.

3.1 Intrinsic signal optical imaging

3.1.1 Acquiring functional maps of neuronal activity

Neuronal activity can comprise the generation and propagation of action potentials, postsynaptic ion fluxes and potentials, neurotransmission, synaptic vesicle recycling, among other processes allocating cerebral cortex energy, along with the maintenance of glial and neuronal resting potentials. Furthermore, the cortex presents activity evoked by sensory stimuli or motor processes, but cortical populations of neurons also show spontaneous coordinated patterns of spiking activity, non-related to any sensory input or motor output.

In regards to the evoked activity, investigating the organizational and functional architecture of the sensory brain requires the means to both detect neuronal activity and to relate these responses to the external stimuli that the subject receives.

The classical approaches developed to this end study animal's brain's *in vivo* by exploring electrophysiological principles: by placing electrodes inside the individual's scalp, one can extracellularly record single cells' electrical activity in a direct manner and access neuron's voltage fluctuations. Multi-unit recordings are also possible through this method.

Other techniques include the 2-deoxy-D-glucose (2DG) autoradiographic method [SOKOLOFF ET AL, 1977] to find and measure glucose consumption in the brain. These metabolic alterations are associated to changes in functional activity and thus an acumulation of the radiolabeled 2DG, representing the integrated rate of glucose consumption, marks the activated areas of the brain.

DYES...

However, many experimental goals require extensive simultaneous recordings while these techniques require long combersome experiments to cover large areas of the cortex. Moreover, electrophysiological mapping methods introduce considerable sampling bias in the recordings as well as poor spacial resolution ($1cm$), while 2-DG maps can only be analysed *post-mortem*, allowing only one experimental session per animal, and can only label two stimulus at the maximum.

Imaging techniques such as functional magnetic resonance imaging (fMRI), near-infrared spectroscopy (NIRS) and intrinsic signal optical imaging (ISOI) introduce less invasive means to simultaneously access larger regions of the brain while the subject is being presented to stimuli and also enable longitudal studies by repeated imaging sessions with the same individual animal. These meth-

ods are based on variations of optically measurable properties of physiological processes associated with neuronal activity.

NIRS....

Intrinsic signal optical imaging (ISOI) enables the visualization of alterations in intrinsic optical properties of neuronal tissues, as a response to neuronal activity.

Slow reflectance light signals are intrinsicly relayed from the surface of the striate cortex due to hemodynamic responses[REFERENCES] that correlate with neuronal activity. Neuronal firing induces blood changes - neurovascular coupling - that produce a light reflectance change.

Neuronal activity requires the hydrolysis of ATP and the oxy-hemoglobin (the protein hemoglobin in red blood cells binded to oxygen) molecules in the capillaries provide the majority of the oxygen used to regenerate ATP via glucose metabolism. Thus, an active brain region is associated with a finely localized increase in oxygen demand and thus a local rise in deoxy-hemoglobin (deoxygenated hemoglobin) and a depletion in oxy-hemoglobin concentrations. This is followed by an hemodynamic response of locally increased blood flow in the capilaries and dilatation of the closeby arteries to replenish and sufice the oxygen requirements.

In this neuronally active situation, the hemodynamic response imposes a light reflectance variation, resulting from three major sources: the changes in blood volume, blood oxygenation and light scattering.

The blood volume component of the signal is the least spatially confined of the three factors, but can nevertheless yield alone functional maps, with the injection of fluorescence dyes into the bloodstream [REFERENCE].

The oxymetry signal is used for instance in fMRI techniques that identify the areas of the brain to which more oxygenated blood is being driven to, relying on how the magnetic properties of more and less oxygenated blood differ. A $1 - 2s$ delayed rise in oxygenation is associated to more active cells and brain usage. However, depending on the magnetic field intensity, this technique can have limited spatial resolution, as it relies on the transition phase that is also associated with the dilatation of arterioles adjoining the original activity sites which can cause signal artifacts.

On the other hand, light scattering changes (REFERENCES) allow for precise temporal and spatial functional mappings of neuronal activity. Higher neuronal activity increases light scattering due to factors like (REFERENCES COHEN 1973). This increase peaks within 2-3 s of the stimulus onset.

With these physiological events optical properties' changes, one can extract the optical signals that correlate with that variance and thus with neuronal activity. Since about 13% of the energy consumption is used for maintenance of the resting state and the greater parcel of the cortical metabolized ATP costs are for action potential propagation (about 47%) [REFERENCES], with the remainder for processes related to synaptic transmission, the intrinsic signal has the major contribution from an oxymetry factor that relates to those inhibitory or subtreshold excitatory input processes.

3.1.2 Intrinsic Signal Optical Imaging: the technique

In the technique used in this work, ISOI, the signal brings about information on the oxy-hemoglobin concentrations during neuronal activity. This method is utilized as one of the best balances in spatial resolution and simultaneous coverage of different brain areas.

Illumination by a stable output source at the red wavelenght level of $540nm$ optimally excites the oxygenated blood flow, while the de-oxygenated blood reflects less light at this wavelength [REFERENCES].

These differentiated properties enable the mapping of the most active, de-oxygenated brain areas at the time of the initial local deoxy-hemoglobin increase, since these regions will reflect less red light than the inactive, amply oxygenated cerebral areas.

ISOI utilizes this principle in brain areas which can be reached by light (around $500\mu m$ maximum). In an animal with a window implantation and illumination of its primary cortex surface, one can record the brain area with a charge-coupled device (CCD) camera to monitor the changes in the reflected light signal from each region of the primary cortex of the subject while this animal is presented to stimuli. In this way, one obtains maps that make correspond the stimulation that the subject receives - visual, somatosensory, auditory [REFERENCES]- to the observed refleted light signal profile at that time interval and in that brain region, whitin some relatively high temporal ($80ms$) and spatial resolutions (in the order of $100\mu m$) [REFERENCES].

For both anesthetized and awake animals, the typical ISOI signal follows a tri-phasic structure: An initial dip, a negative peak at about 4-6s after stimulus onset, and a large rebound [GET REFERENCES].[GET IMAGE]

The signals' information is extracted by calculating differences between the reflectances of the imaged brain area at unstimulated baselines and post stimulation time points. For each stimulus, multiple repetitions are held and the respective signals averaged across the same time points.

Furthermore, in regards to the stimuli dependence of the signal's timecourse, the ISOI signal can be divided into a global stimulus-non-specific response and a local stimulus-specific response that is observed from functionally organized cortical columns[REFERENCE]. This latter component stands as the actual mapping signal.

The properties of the ISOI signal in amplitude and temporal dynamics, as well as of its components, depend on both the stimuli and on the wavelength of the ilumination light that the brain is receiving[REFERENCES].

A green light source at 546 nm is found optimal for obtaining an initial image of the brain surface and its blood vessels. On the other hand, a red light at 630 nm mostly translates changes in blood volume and oxygenation and can thus convey the dynamics of neuronal activity, while the animal is being stimulated.

The figure obtained with the green light can be later overlayed with the mapping image obtained with the red light under stimulation. This overlayed image then relates the neurons' activity specification with the vessels anatomy, serving as a functional map. [GET IMAGES]

Furthermore, [REFERENCE] found that the signal's rise time and time to peak were nearly identi-

cal for both short and long stimulus durations. However, the relaxation time course of the signal does depend on the stimuli duration, which imposes an appropriate inter-stimulus interval and/or aware analysis.

3.2 Calcium indicators and transgenic lines

In the experimental efforts of this project, there's need for large-scale recordings of neural activity. A myriad of different indicators has been presented in literature and used to divergent extends, being that the suitability of each method to each experimental configuration varies with the priority weights given to factors as the neural events detection fidelity, the specificity of the expressed cell types, and the aimed recording's temporal resolution.

In transgenic mice, given neural processes can be marked and visibly expressed. Genetically encoded indicators of neural activity (GEAIs) are optical indicators that allow for observations that cannot come from electrodes or functional magnetic resonance imaging, accessing neuron's populations' dynamic evolutions over time, within a simultaneous, non-intrusive and less biased observation.

A way of accessing the synaptic excitation occurrence is by means of calcium indicators. Ca^{2+} regulates the fusion of synaptic vesicles: Presynaptic terminals contain voltage-gated Ca^{2+} channels (VGCC) in their membranes and their opening occurs when excited by a presynaptic action potential that results in the influx of Ca^{2+} which triggers neurotransmitter release. This influx also happens as action potentials propagate throughout the neuron. In this way, the calcium entry amplifies the marker of neural activity that is wished to detect, by transforming the transient events in the presynaptic membrane into biochemical more prolonged and more widely localized changes.

However, some limitations restrain the use of this sort of indicators: The temporal precision of the process is limited, as the involved half-decay times can be long: In different family's of GECIs, a trade-off emerges between the signal's responsiveness' strength and it's temporal accuracy.

In the current project, a suited GECI was selected from the ultra-sensitive GCaMP6 series [**?**]. GCaMP consists of three main components: circularly permuted green fluorescent protein, cpGFP, the chromophore, that is, the region that determines the colour of the compost; calcium-binding protein calmodulin, CaM, and CaM-interacting M13 peptide. Through mutagenesis of this compound, optimizing for sensitivity, GCaMP6 was selected. Besides its great sensitivity, GCaMP6 indicators allow the reliable detection of individual action potentials, the imaging of large neuron populations and small synaptic compartments, all over long time scales. There are GCaMP6 variants suited for different applications, with several overall brightnesses, rise and decay kinetics and calcium affinity properties.

The expression of this compound could be achieved by viral gene transfer using adeno-associated viruses (AAVs). However, besides introducing some level of invasiveness, this method produces different degrees of expression in neurons accourding to their distance to the infection site as well as a continuing increase of expression over time until possible damage to the cells, limiting the imaging time interval of opportunity. These disadvantages can be obviated by transgenic expression of GECIs. The mice that will serve as subjects in this thesis project were genetically modified as to express GCaMP6 in

most neurons of the cortex under the Thy1 promoter [**?**].

GCaMP6 increases green fluorescence in the presence of calcium. As a released neurotransmitter or an action potential opens a VGCC, entering calcium induces the biding of calmodulin (CaM) to a peptide (RS20, homologous to M13). This causes the repositioning of Arg337 (in the CaM domain) which in turn leads to the protonation (loss of a proton) from the chromophore. As the acid dissociation constant decreases, this conformational change of the chromophore induces an absorbance shift and, upon blue excitation, green emission is increased.

3.3 Imaging techniques: Two photon laser-scanning microscopy

Investigation of neuronal activity often requires access to deep layers of brain tissue, without compromise of the entire brain structure and while preserving the remaining more superficial layers. Deep ($> 500\mu m$ below the brain surface) optically sectioning in highly scattering tissue, minimally invasive techniques such as two photon laser-scanning microscopy (TPLSM) present an effective solution.

Moreover, neuronal phenomena can be relevant in broad scale ranges, both spatially and temporally. TPLSM presents images with submicron lateral resolution, micron axial resolution and millisecond timescales, appropriate for many neuronal processes, in particular for observing GCaMP6s expressing neurons in V1.

With high resolution, sensitivity, contrast and being able to track events over large cortical ranges, two-photon excitation laser-scanning microscopy provides a way of accessing fluorescent objects, such as the GCaMP6 expressing neurons, by selectively exciting them and detecting the produced light signal. This technique can furthermore be applied to living or intact tissue, with minimal photodamage (phototoxicity and photobleaching). The probability of detecting a signal photon per excitation event is greater than with previous techniques, especially for imaging deep in scattering tissue.

Here, we review other fluorescence imaging techniques that preceded TPLSM and follow with the technical main concepts in the assemblage of a TPLSM system and its optical theoretical fundamentals. The presented functioning principles can aid in the understanding of TPLSM advantages, justifying its use in the research subject of this project, and also serve as an overview of the main possible tools often used in experimental neuroscience imaging research.

3.3.1 Single-photon Imaging

Fluorescence microscopy makes use of either artificially introduced or intrinsic molecules in a biological preparation that can be excited by light at a wavelength within these molecules' linear absorption spectrum.

In single-photon imaging, as appropriate light is shined over a preparation, a photon can be absorbed by the molecule, exciting it to a higher electronic state. Then, upon relaxation back to its ground state, the molecule will emit a photon at lower energy and longer wavelength than the excitation light.

Regardless of the focusing of the beam, the fluorescence throughout an entire plane at the same axial coordinate (perpendicular to the incident excitation light) will be virtually constant: The probability of an excitation process (absorption of a photon) is linearly proportional to the excitation light intensity

(number of photons incident per unit area). As one approaches the focus of the excitation bean, the light intensity increases as there is less cross-sectional area to distribute the power over, but, in the same proportion, there are also less molecules to excite in that same cross-section. Thus, the fluorescence excitation in single photon imaging results constant across the entire axial reach of the excitation light beam.

3.3.2 Direct Imaging

In direct imaging techniques, or whole-field fluorescent microscopy, the full region of interest is illuminated with excitation light and all of the consequent fluorescent light is collected.

This method allows high data collection rates, depending on the array-detector technology available. However, since the fluorescence origin is not distinguished and out-of-focus planes contribute non-uniformly to the background levels read in a focused plane, axial resolution suffers, as well as signal-to-noise (STN) levels, in relation to more processed techniques.

In fact, adaptations of this technique explore the elimination of out-of-focus planes' fluorescence, by various methods:

- deconvoluting images from immediately above and bellow planes from the target images of the focused plane, modelling and subtracting this out-of-focus light from the background levels.
- projecting a vibrating grating in the preparation plane, with a spacing on the order of the lateral diffraction limit, and using its modulation in time to extract the part of the signal that is concurrently modulated and that thus corresponds to the target plane.
- using an interferometry cavity to produce an optical field varying axially and distinguishing in this way the signal coming from each axial plane. However, this method can only be applied in thin preparations.

3.3.3 Confocal laser-scanning microscopy

Laser-scanning microscopy presents better axial resolution than direct imaging. Conversely to direct imaging, in confocal laser-scanning microscopy the light source focuses the excitation light in a target focal volume, instead of illuminating the full region of interest.

Typically, a laser is focused on a given target plane and scanned over the sample. When an excitation occurs, it is detected by photodetectors. These responses are then summed over some microseconds and mapped to single pixels of an image.

An incoming collimated laser beam is deflected by two perpendicularly placed rotating mirrors and then focused by a microscope objective onto the biological preparation, in case, a mouse's V1 *in vivo* brain layer.

The rotation of the two mirrors generates a trajectory in the laser's focused spot in the animal's brain, under a given raster pattern across the region of interest. Then, the fluorescent light produced at the focal volume is collected by a detector as a function of time. Typically, the fluorescence responses are summed over some microseconds corresponding to the time spent by the laser focus at that position

and mapped to single pixels of a final raw image : the fluorescence time series is therefore transformed back in the fluorescence function of the corresponding positions in the brain's scanned area.

Limited to the speed and reliability of the rotating mirrors' angular deflection movement, this method has the disadvantage of reduced acquisition speed compared with direct imaging techniques.

The axial resolution is improved by preferentially collecting signal from the focused volume and rejecting light coming from out-of-focus planes: The fluorescent light is refocused along the same path as the excitation laser beam and, after being deflected by the scan mirrors, this light is spatially filtered by a pinhole as to only pass light signals from radius corresponding to generation from the illuminated region of the brain. For this reason, this method is only efficient for optically thin preparations: If the light beam is strongly scattered, the pinhole will block deflected beams that in fact originated from the focal volume, and collect deflected light from outside the focal plane, decreasing the STN ratio.

3.3.4 Two photon laser-scanning microscopy

In TPLSM, the laser beam light is at twice the wavelength and half the energy of the light used in one-photon microscopy. Thus, lower-energy photons (deep red and near IR) are sent by a focused laser to a fluorophore unit and can excite, in simultaneous combinations of two, the higher-energy electronic transition required for the emission of fluorescent light. Two photon simultaneous absorption is a nonlinear process, as the absorption rate depends on the squared value of light intensity. This intensity drops quadratically with the distance from the focus. Therefore, if the numerical aperture objective is small enough, this excitation is localized, and the excitation can affect a very small focal volume and produce good 3D contrast and resolution.

In fact, in TPLSM, the total fluorescence generated in a cross-sectional plane, F_{tot}, is proportional to the square of the laser beam intensity, I^2, and the illuminated area, A. Thus, with P the incident laser power and $I = P/A$, considering that the illuminated area in a given plane scales with the square of the axial distance from that plane to the focal plane, $A \propto z^2$, for z larger than the confocal length, we obtain:

$$F_{tot} \propto I^2 A \propto \left(\frac{P}{z}\right)^2 \text{ for } z \geqslant z_{confocal} \tag{3.1}$$

with

$$z_{confocal} \equiv \frac{1}{2\pi}\frac{\lambda_o}{n}\left(\frac{n}{NA}\right)^2 \tag{3.2}$$

where n is the optical index of the preparation, λ_0 the laser's peak excitation wavelength and NA the numerical aperture of the objective.

The integrated fluorescence over $z \geqslant z_{confocal}$ is given by:

$$2\int_{z_{confocal}}^{\infty} dz F_{total} \propto 2\int_{z_{confocal}}^{\infty} dz \left(\frac{P}{z}\right)^2 \rightarrow constant \tag{3.3}$$

and the relevant contributions to the collected fluorescence are therefore only from the light within a focal depth $z \geqslant z_{confocal}$, regardless of scattering.

On the other hand, with the single-photon technique, $F_{tot} \propto IA$ for $z \geqslant z_{confocal}$, and the integral diverges:

$$2\int_{z_{confocal}}^{\infty} dzF_{total} \propto 2\int_{z_{confocal}}^{\infty} dzP^2 \to \infty \tag{3.4}$$

Another asset of 2PE methods are its features with scattering processes.

As photons enter tissue in a preparation, they scatter and deviate their paths according to inhomogeneities found in the refractive index of the medium, and this reduces the amount of light both delivered to the focus and emitted from the fluorescent molecule to the detection apparatus. The size of a scattering particle can be parametrized as the elastic scattering length $x = \frac{2\pi r}{\lambda}$, with r its the characteristic length and λ the incident light wavelength. The scattering length corresponds to the length over which an incident light's deflection can be neglected.

In summary, 2PE presents four main advantages in this regard, being specially suited for optically thick preparations:

- The TPLSM technique uses near IR beams. These wavelengths penetrate tissue with less scattering than visible waves as those used in one-photon microscopy. In this way, 2PE methods deliver excitation light to deeper layers of the preparation more effectively. Furthermore, these waves are less absorbed by biological tissue than blue or UV light.

- The non-linearity of 2PE, with the amount of fluorescence generated in an axial plane quadratically decrementing as a function of the distance from the focused plane, also contributes to the reduced collection of scattered photons coming from out-of-focus planes, which would worsen the STN ratio;

- Since the excitation is localized, in principle all the fluorescence photons coming from an excited molecule, even if scattered, portray useful signal, not being lost and not contributing to background noise.

- Not requiring spatial filtering of the fluorescent beams, a higher collection efficiency is possible for scattering tissue than with confocal microscopy.

Another important characteristic of TPLSM is that with this method the excitation and fluorescence light spectral peaks are separated further than with other techniques, since twice the energy of the fluorophores de-excitation must be delivered by the laser. This simplifies the technicality of distinguishing these light beams. Furthermore, the fluorophores have more energy levels available for absorption, producing a broader spectra of emission light with a single laser source. This allows simultaneous collection of different wavelength fluorescent light, with separated channels revealing the fluorescence behaviour of different molecules. This can be used for simultaneous imaging of neurons and axons, distinct markers and dyes, or multiple genetically induced compounds.

Since the probability of simultaneous absorption of two photons is smaller than single-photon absorption at twice the energy level, the lasers used for this method should be powerful enough to compensate for the small two-photon cross-sections and produce sufficient signal levels. Moreover, the

average power levels delivered by the laser should avoid thermal damage of the preparation. Considering that 2PE efficiency and depth penetration increase as the instantaneous power delivered by the laser, hence with the inverse of pulse duration, the device should thus be suitable for short light pulses $(10 - 100 fsec)$. Mode-locked Ytterbium-doped and Cr:forsterite lasers suffice these requirements for the considered wavelengths.

Objectives are used for the essential focusing of the laser beams. Another important consideration regards the detectors: These should cover large sensitive areas (millimeters), as well as contemplate good gain, quantum efficiency, and other important thresholds, depending on preparation being imaged. Photomultiplier tubes (PMTs) are usually applied for this purpose.

TPLSM resolutions, both in depth δz and lateral δr, depend on the confocal length of the system:

$$\delta z = 4\pi z_{confocal} = 2\frac{\lambda_0}{n}\left(\frac{n}{NA}\right)^2 \tag{3.5}$$

$$\delta r = 1.2\pi\frac{NA}{n} z_{confocal} = 0.6\frac{\lambda_0}{n}\left(\frac{n}{NA}\right) \tag{3.6}$$

In the case of the performed experiments, the laser's light was filtered for $\lambda_0 = 920nm$, the brain tissue preparation's optical index can be approximated to ??? and the objective's numerical apperture was [SPECIFICS ON THE OBJECTIVE] NA =???. This gives $z_{confocal}$ and the resolutions λz =??? and λr =???. A beam can only be focused as long as $x >> z_{confocal}$. Since in living mouse's neocortex x $200\mu m$, TPLSM's beam focus is again virtually not affected by scattering, deeming laser power the only practical restriction for the TPLSM technique.

Photodamage of the nervous tissue and photobleaching of the fluorophores during TPLSM sessions are localized effects whilst in single-photon these effects endure throughout the full light penetrated depth. Furthermore, these effects in TPLSM have been reported to have been increasing at the focus in a non-linear manner with exposition time and light source intensity[REFERENCES]. Thus, regarding the previously discribed strong advantages for TPLSM versus single-photon imaging, for thin preparations, a preference between single- and two-photon imaging techniques is not clearly resolved.

Regarding the selected light source's efficiency, the spectral width of the pulsed laser beam $\Delta\lambda$ should be within the fluorophore molecules' two-photon excitation spectrum. This is given by:

$$\Delta\lambda \ \frac{\lambda_0^2}{c\tau} \tag{3.7}$$

with λ_0 the laser beam's peak wavelength and τ the temporal width of the pulse.

For GCaMP6s mice, the proteins absorb optimally at 920 nm. Therefore, the laser beam is set at this peak value and with this being a Ti:Sapphire-based system, temporal widths reach about 10 fsec, producing a wavelength width of ????, less than the 80nm absorption band with of GCAMP6s fluorophores, VALUE, as desired.

PUT SCHEME

4

Technical Implementations

Contents

As the first part of this thesis' work development, hardware adaptations were implemented and software protocols were programmed for the real-time behavioural control and stimulus presentation to be used in the experiments. This was done with the open-source arduino-based system Bpod, by adapting the previously used microkernel-based system Bcontrol. This required the development of a synchronized graphical user interface, the communication between a governing machine, a microscopy apparatus, a stimuli monitor and a bpod device, within minimal processing time, as well as different states matrices and protocols for each type of visual stimulation display - RF mapping, tuning mapping and SM properties investigation. Moreover, the system also required proper functionality within the software controlling the two-photon microscope, which was enabled by the trigger and configuration settings of the software ScanImage.

4.1 System's scheme

The experimental procedure of visual stimuli display involved four main components in communication of parameters, configurations and triggered synchronization: A governing machine and a stimulus display matlab instances, a Bpod device and the set of two-photon laser microscopy appliances and software.

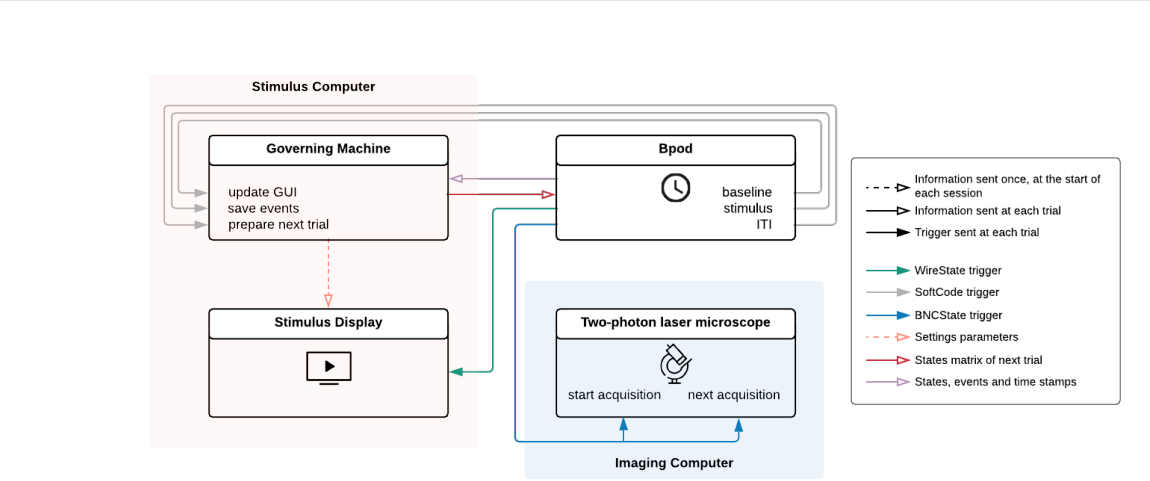

Figure 4.1: Setup and connections scheme of devices used for stimuli presentation and real-time imaging.

Controlled by one of the computers, called here stimulus computer, were the governing machine and the stimulus display.

The governing machine held the Graphical User Interface (GUI) as well as all of the computations and running protocols with Bpod's software for saving the stimuli settings and preparing the stimuli configurations and states matrices for the different trials.

The stimulus display was produced in a second monitor connected to this stimulus computer and operated within a second matlab instance of routines coded with Psychtoolbox software for interfacing between Matlab and the computer screen. This Matlab instance loaded, at the beginning of the session, all of the stimuli settings that were saved in the bpod's Matlab instance. With a counter, the script iterated the full trials structure, displaying the applicable stimuli at the proper times. This timing

synchronization was enabled by triggers received in a NI-DAQ data acquisition board.

The bpod apparatus produced these triggers, connected to the system and taking advantage of a precise internal clock. Having received each trial's state-matrix specifications from the governing machine with enough buffer time, bpod produced the appropriately timed states - the main ones being the baseline, the stimulus and the ITI - and sent the required triggers at each stage. At each trial, in the beginning of the baseline period, a trigger was sent to the governing machine to update the GUI to show the current trial stimuli specifications; during the stimulus presentation, another trigger was sent to save the events of the previous trial and during the ITI an instruction was sent for the governing machine to prepare the next trial by computing the next states matrix with the new trial's stimuli configurations. Bpod also sent, at the beginning of the stimulus display state, the trigger for the stimulus computer second matlab instance to display the loaded and prepared stimulus in the screen visualized by the animal. Finally, at the beginning of the baseline and in the end of the ITI of the proper trials, a trigger was sent to the called imaging computer that held the software controlling the two-photon laser microscope for respectively starting and afterwards completing and proceeding to the next brain scanning acquisition.

The two-photon laser microscope held different components: The laser apparatus with the mirrors, lenses, beam-splitter and remaining light path enforcers; the objective enabling both a bright field and a two-photon configurations; the synchronization device BLACK BOX[?], a NI-DAQ data acquisition board for receiving Bpod's triggers, and finally the imaging computer that operated the controlling software application ScanImage 4 for laser scanning microscopy. This was also the computer that saved the raw image sets acquired from the two-photon scannings at each protocol session.

The sent information and triggers used the different physical wiring possibilities: Firstly, SoftCodes were sent from bpod to the governing machine's computer, via the USB port that connected these devices. From bpod to the stimulus display NI-DAQ board, WireStates were used, and, to the two-photon NI-DAQ board, BNCState triggers were sent. On the other hand, the information about states, events and trial time stamps was sent at each trial via USB from the Bpod device to the bpod's governing machine matlab instance and then saved with its own software. From the governing machine, information was sent as the following trial's state matrix, to the bpod device also via USB and the next trial's settings were sent to the stimulus display matlab instance by saving them at the beggining of each protocol session in a file that was then loaded in the stimulus display matlab before starting the session.

4.2 Bpod

4.2.1 Motivation and previous system

Bpod encompasses a flexible open-source platform for developing stimuli presentation, behavioural protocol and reinforcement experiments. The system builds on a parallel processing model, software functions are written in Matlab/Python and the firmware builds on Arduino language. The system was devellopped in Kepecs Lab [REFERENCES] at Cold Spring Harbor Laboratory and is currently maintained by Sanworks LLC, a company focused on open source neuroscience tools.

The main capability of the system is its precise time measuring feature. In imaging and even more so in electrophysiology animal experiments, it is paramount to control and synchronize the timings of stimuli presentation, behaviour/neuronal activity detection and states sequencing in the different setup compontents. Precise triggers from a governing machine to a brain activity measurement device - the two-photon setup, in this case -, to a stimuli display - visual or not - or behavioural gadgets allows reliable functional brain mappings, and appropriate analysis and interpretation of an animal's brain or physical responses.

Prior to this implementation, the Cortical Circuits Lab was using B-control for mice's behavior measurement and finite states machine, a system developed by Brody Lab at Princeton University [REFERENCES]. In fact, Bpod builds on B-control's parallel processing design idea: the state machines for each trial are constructed in Matlab in a governing machine and executed in a separate device. For B-control, this is a separate microkernel real-time Linux computer. Bpod, on the other hand, uses an Arduino microcontroller network with finite state machine firmware for the real-time processing. This provides higher level software tools for adapting and constructing protocols, as well as a simpler, less expensive hardware solution.

Bpod entails two items: The device that provides the state machine substract, with a precise internal clock, output ports for TTL triggering, input ports, behavior ports with infrared photogates, LEDs and solenoid valves for dispensing liquids; and the software that, run in the governing machine, provides functions with which to code the states matrix, to equip the system with a GUI and the necessary supporting functions for each protocol and to implement functioning communication between the Bpod device and the other components - in the case, the stimuli computer and the two-photon computer.

The Bpod system presents the following five principal functionalities:

- Ensures the precise triggering between the Bpod device and the involved components - microscope set, stimuli screen and governing machine;
- By enabling the implementation of a GUI interface, this equips the user with a practical way of setting the characteristics of the stimuli at the start of the experimental session;
- The GUI also facilitates the monitoring of the stimuli presentation sequence at the same time as it is happening in a given session: the current trial with its correspondent stimuli properties is shown, as well as the appropriately timed states - baseline, stimuli presentation, ITI and auxiliary states - within the running protocol. Moreover, the states machine can be started - with the last submitted stimuli settings -, stopped, paused, continued or restarted by the user at any time, keeping the synchronization and . [GET IMAGE]
- Automatizes the saving of the data structures containing a session's stimuli sequences, as well as the time stamps related to the state matrix that was run, with the computer times for the start of each state or event leading to a state change.
- Although not used during this work, as the experiments only regarded stimuli presentation, and

because the animals were kept anaesthetized, minimizing the need for further controls, one of Bpod's main functionalities regards the measuring of the animal's behaviour. The state machine receives these discrete behavioral events and can rapidly respond by changing the animal's environment. For instance, by connecting Bpod to treadmills, one can measure a small animal running behaviour; by connecting Bpod's appropriate ports to water valves connecting to drinking tubes, those can be controlled for implementing a reward system during reinforcement experiments; Bpod also detects the instant when discrete events happen. This can be used for example in decision making experiments: a snout entering a port or a tongue blocking a photogate can indicate an animal choices. High quality audio stimuli can also be produced with the integration of Psychtoolbox. These features deem the Bpod system a practical tool for various behavioral paradigms: two alternative forced choice (2AFC), go/no-go decisions, reaction time measurement, self-stimulation (repetition of physical movements), social value measurement, among other possibilities.

The access to these functionalities is to be understood as provided that the user develops the programming protocols and optimizes it to meet the requirements that the experiment entails. Bpod system is not a ready to use package: it requires an understanding of the functions provided, Matlab or Phyton coding, and all of the hardware communication specifications in each protocol's case. More fundamentally, the user should have a clear planning of the specific communication scheme to use in their case, as well as of the GUI and states machine development and the important variable structures with the information to be produced, exchanged between components and saved. Documentation is available in [BPOD WIKI] and technical support can be found in the cooperative [BPOD FORUNS].

The development process started in a 45-days internship at the Cortical Circuits Lab in 2016, in which l adapted a stimuli presentation protocol from Bcontrol to Bpod, by familiarizing with both Bpod and B-control syntaxes and function environments. This work was carried with the mentorship of Leopoldo Petreanu and the guidance of Tiago Marques through the B-control environment protocol that he had developed and that the Laboratory had been using. The protocol enabled full-screen moving gratings or random dots, under different stimuli properties - timings, screen stimuli positioning, number of repetitions, luminosity values, gratings versus random dot stimuli type probability, orientation, direction, dots speed, density, coherence and size, gratings temporal and spatial frequency - in pseudo-randomized selections according to a general user's requirements with the possibility for fixating a seed, facilitating troubleshooting. At the time, this protocol was tested with the same stimuli Psychtoolbox code written for B-control. Since then it was further used in electrophysiology experiments in the Laboratory by the PhD student Gabriela Fiorze.

In this thesis' protocols development, I used this previously coded and tested protocol as a basis. However, in this case, besides having to adapt the states machine, GUI, main and support functions from the governing machine, it was also necessary to develop new stimuli protocols with Psychtoolbox [REFERENCES] and to understand the triggers, ScanImage software [REFERENCES] and hardware connections made with the two-photon computer setup. Furthermore, at the time I used a Bpod State Machine device at version 0.5 that was switched at this point for version 0.9, with slight differences in

hardware, as well as in the software functions and firmware.

In the following chapters I will go through the three protocols I developed for this thesis' experiments. For these, as in the originally developed Bpod protocol, I focused on the protocols user-friendliness, minimal processing time and in the flexibility of the code for both other similar experiments and for adaptations to other paradigms.

4.2.2 Bpod Hardware implementation, specifications and alterations

The Bpod State Machine device runs on a Arduino Due 32-bit processor with 84MHz clock speed. The bill of materials can be found at the device's wiki [REFERENCES].

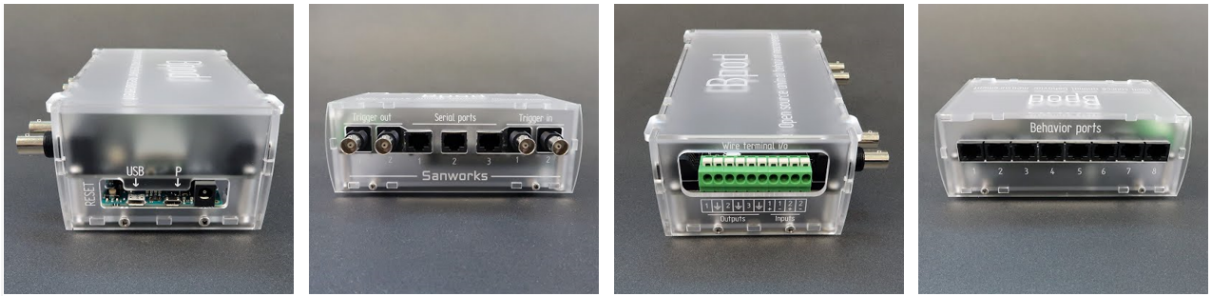

Figure 4.2: Perspectives of Bpod State Machine device version 0.5, identical parts as in version 0.9, but with fully transparent box container design. Images from Sanworks Bpod wiki page [REFERENCES].

Firstly, the device contains a 'reset' button to reset the device if necessary and two USB port jacks - an Arduino's native USB port to connect to the governing machine and a programming port for cases when it is necessary to re-upload Bpod's firmware. Moreover, there also is a power barrel jack for cases when the USB port is not supplying enough power to the device - this power jack was used in troubleshooting but, with the final setup, the power from the USB proved to be enough.

In Bpod, there are four BNC channels, two input and two output. The output channels are constructed to serve as 5V triggers, as Bpod can produce events and send triggers with TTL logic through them. These were initially used here to connect to the two-photon computer's NIDaQ board, one of them as a 'start acquisition' trigger and the other as a 'next acquisition' trigger.

Bpod also has bare wire terminals, with TTL logic. The spring terminal channels are of two inputs (2.5V to 5V) and three outputs, all with the respective grounds. The outputs here are 3.3V TTL pulses. In this thesis work, I required one extra trigger port to be connected to a NiDAQ [THE WHITE THING]. This WHITE THING was by its turn controlling the stimuli screen. One of these wire channels was thus used to portray trigger pulses. For this, to be assured that there was sufficient voltage at this port (5V, according to the WHITE THING specifications [REFERENCE]), the Bpod circuit was altered in the Champalimaud Foudation IT platform with a 3.3V to 5V voltage amplifier at this wire output channel [HOW? CHECK].

Although not used in these experiments, the apparatus additionaly contains behavior study components: An ethernet that can connect to a lickometer or a nose port, as well as 8 behavior ports, each with an LED with software-adjustable intensity, a solenoid valve (12V, 150mA), and an infrared photogate. Also not necessary for these experiments, the device also contains serial ports that allow

to connect it to other Arduino boards or modules that can be acquired from the same company.

4.3 Software: Governing machine protocols and stimulus presentation

Bpod's software allows to load user-made protocols and run them within the built-in bpod interface, joined with the protocols' specific GUI windows (IMAGE).

In this project, three protocols were developed for different ends: receptive field mapping, tuning measuring and studying the spatial structure of surround modulation.

Each of these were subsequently used in mice experiments. The produced data was also analysed, validating the method and tool in the three protocols.

The RF protocol served to find the RF positions after each experimental session and assess if the majority of the measured cells' RFs was centred at the corresponding display monitor center, as desired. Specifically, the obtained RF maps either indicated, in combination with the retinotopy maps, in which directions one should move the objective to correct the imaging position in following sessions or confirmed that the objective and mouse placing was appropriate (SEE CHAPTER). Furthermore, this data was also combined with the SM protocol's results for RF position-dependent analysis of the SM effect (SEE CHAPTER).

The tuning protocol was implemented to measure the selectivity of cells in a flexible array of conditions. The data collected from this protocol was analysed and some cell's tuning behaviour examples are shown in (SEE CHAPTER). This analysis served to validate the protocol and aided in troubleshooting the SM analysis. Moreover, this protocol was also used to find the RF centred imaging positions during experiments.

Finally, the SM study was the main focus of this project's experimental component, and the obtained results are presented in (SEE CHAPTER). The implementation of this protocol allows the presentation of any configuration with center and surround moving gratings' patches, in any combination of the four cardinal plus center positions. For this project's purposes, 124 were chosen, in a given set of grating frequencies and stimuli sizes (SEE CHAPTER).

Each of these protocols follows a similar structure of five files, each with different case functions:

- **main**: initiate, submit, start, prepare next trial, synchronize GUI, save settings and events, process trial completed, restart and stop;
- **states matrix**: prepare matrix, run;
- **GUI**: initialize, synchronize;
- **SoftCode handler instructions**: maps SoftCode bits to be sent in the states matrix to functions: main(prepare next trial), main(save settings events) and main(synchronize GUI);
- **Support functions**: set session, set next stimulus and save parameters.

In bpod's built-in interface, one can set the mouse ID, load the settings to use as default and then call the desired protocol.

At this point, the main file is called to initiate the protocol: This by its turn calls the GUI initiation function, which initializes the settings variables in a global structure S, in different fields according to the required type of GUI to be used (an edit box, a toggle button, a slider, an edit array, an array display or a push button). This organization allows to then easily initialize handles of each parameter's user interface control, depending on the type of GUI (IMAGES).

In the ScanImage interface at the imaging computer, the appropriate configurations must be set by the user before starting the stimuli and bpod protocol - The user must choose the number and positions of the imaging planes, imaging trigger ports, brightness of the brain recordings displayed, as well as the path and name for the recorded movies. Then, the imaging system can be instructed to await the external triggers that will come from bpod.

In bpod's computer, once the user chooses the intended parameter values in the GUI and clicks the *submit* button, the GUI is synchronized, the current trial variable is set to 1 and three support functions are run on S:

First, the session is set: An angular coordinate system is computed, converting monitor (y, z) coordinates in azimuth and elevation, from the perspective of the mouse:

$$elevation(^{\circ}) = -\left[\frac{\pi}{2} - \arccos\left(\frac{z + z_0}{\sqrt{d^2 + (y + y_0)^2 + (z + z_0)^2}}\right)\right]\frac{180}{\pi} \tag{4.1}$$

$$azimuth(^{\circ}) = \frac{\arctan(y - y_0)}{d}\frac{180}{\pi} \tag{4.2}$$

with y_0 and z_0 the positions in respectively the horizontal and vertical monitor axis centred perpendicularly to the mouse's gaze and d the distance from the mouse's eye to the center monitor position.

In the RF case, grid positions can be produced from the settings and randomly permuted in a presentation sequence, along with a key for the respective gratings direction sequence also in pseudo-randomized order.

Similarly, for the Tuning protocol, all of the possible combinations of center azimuth, center elevation, stimulus size, temporal frequency, spatial frequency and moving gratings direction are randomly permuted, within the total number of trials, with the specified number of repetitions for each trial type. This maps a pseudo-randomized sequence for every dimension of stimuli properties that is saved and displayed in a GUI variable.

Finally, for the SM protocol, every trial type is also repeated a specified number of times, put into an array that is then shuffled and creates a complete order of stimuli presentation. Each value in this final array corresponds to values in other variables that are also saved and displayed: these represent if the center, left, right, top and/or bottom patches are being presented, and if so what are its gratings directions.

The second support function sets the next stimulus, by updating the current stimulus variables to the first trial case, according to the order in the total stimuli properties arrays created (position and direction sequence for the RF protocol, for example).

Then, in the third support function, the relevant parameters for the stimuli graphical presentation are saved in an external *next stimulus* file, to be read and loaded in the psychtoolbox stimuli display Matlab instance.

The GUIs are synchronized to the newly computed values of the parameters, and the first states matrix' preparation is called.

The matrix sent to the bpod device follows the flowchart in figure 4.3.

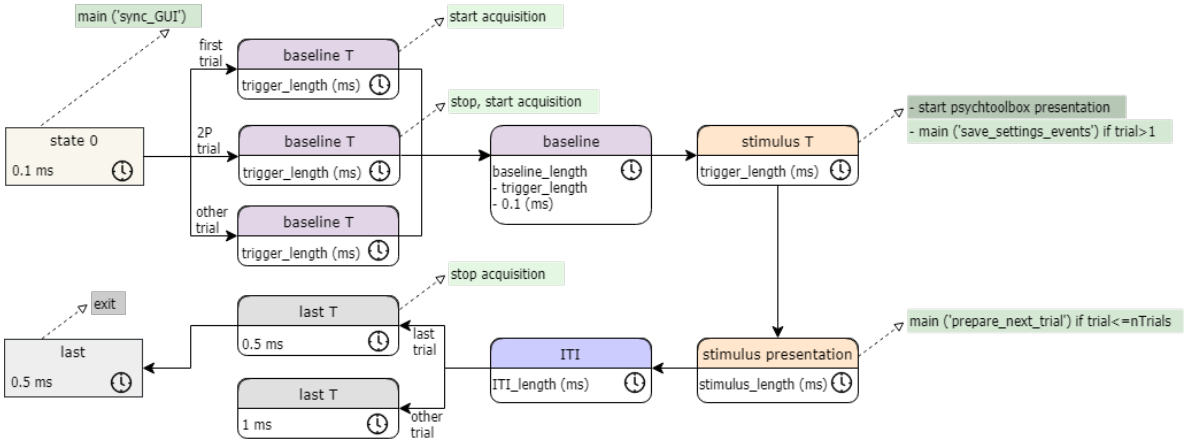

Figure 4.3: Flowchart of the states matrix implemented for the three developed protocols (RF, Tuning and SM). Each state is represented by a name, a timer, state change conditions and output actions. The states machine is formed by three principal states: a baseline, a stimulus display and an ITI. Trigger ("T") states were added, with *trigger length* times corresponding to the duration of the according pulse. All of the state changes were to happen at the end of the internal timer at the current state. The output actions are represented by dashed arrow lines: these represent triggers to the imaging computer (lighter green) through BNC connections, to the NIDAQ of the psychtoolbox matlab instance (darker green) through a wire connection and internal triggers to other functions in the governing machine, through USB connected softcodes (medium green).

After this *submit* process, the user can initiate the psychtoolbox script written for the given protocol at use, in a second matlab instance. This script opens the NIDAQ device and configures it to receive triggers, then opens the screen in the setup monitor in front of the mouse, and loads the session settings in the *next stimulus* file.

In the case of the RF protocol, this computes a checkerboard mask and divides it into a mask for each grid cell's position figure. It also prepares full screen moving gratings at the settings' frequencies and contrast levels, going in the indicated sequenced directions, within a set of frames in the required number for completing the time length of the stimulus presentation, acording to the monitor's frame rate. Finally, these are combined into textures - sequences of images - that correspond to each trial type and that are saved in a structure for that trial type and every frame of that trial.

The preparation of display movies for the Tuning protocol is done in a similar way: Masks are produced for a circular patch with the possibly multiple sizes and centre positions indicated in the stimulus file, and full screen moving gratings are computed in the brightness levels specified, and for the spatial and temporal frequencies at hand, which can also be more than one in the same session. Then the gratings are masked, forming sets of images (textures), each corresponding to a type of trial and saved in a structure.

For the SM protocol, five masks are produced with the sizes and positions indicated, one circular

patch for the center stimuli, and four cardinal quarter-torus for the surround patches. Gratings are drawn at the instructed frequencies and contrasts, also in full-screen. This means that the final textures, maskings of the moving gratings, form in-phase center and surround patches with the same grating properties. These textures regard combinations of the center and surround patches, and each is saved in correspondence to one trial type.

When a trigger reaches the entrance specified in the NIDAQ device, the corresponding trial texture frames are drawn in sequence and the timing between the previous trigger and the current one is displayed on the matlab command window for monitoring possible skipped triggers.

When the textures are loaded, the user can click the start button, which first saves the submitted settings in a stimulus file and then calls the states matrix to run.

Softcodes sent from the bpod device to the governing machine allow processing of given instructions, while the states matrix is simultaneously being run, thus enabling parallel actions.

As represented in image 4.3, in the beginning of a trial, a trigger from the bpod device to the governing machine dictates the GUI's synchronization, updating the displays to the current trial properties. Another softcode is sent, before the stimulus presentation, to save the events and time stamps from the previous trial in a file in the governing machine, in the case of trials after the first. Finally, a *prepare next trial* instruction is sent in the middle of each trial. In parallel to the stimulus presentation, this instruction internally increments the current trial variable, then runs the *set next stimulus* support function and calls the *prepare next matrix* function. This ensures that the next trial variables, GUI and matrix are ready when the current trial finishes and the next *run states matrix* instruction is sent.

During the trials, triggers are sent to the imaging computer to acquire sequenced images of the animal's brain. The user can decide how many trials are added in every recorded set of images, by changing a GUI variable. Thus, at the beginning of the first trial, a *start acquisition* trigger is sent to the two-photon system and then, at the beginning of every first trial of the imaging sequence, a*next acquisition* trigger is sent, to stop the recording of the images in the previous set and a *start acquisition* follows to record the next images in a new set. A displayed variable in bpod is incremented every time these first trials are reached. In combination with a scanImage interface's display of the number of acquisitions held, the user can monitor the synchronization between bpod and the imaging system.

Once the current trial reaches the last state and the current matrix is finished, the main's *trial completed* function is called. This increments the current trial variable and calls the run states matrix function again. The system enters the prepared states matrix, with the variables, GUI and matrix timings and conditions correspondent to the incremented trial.

The recurrent cycle continues until the last trial is completed, in which case the run states matrix instruction is not sent again, the events and trial stamps from this last trial are saved, and the bpod protocol stops.

At this point the psychtoolbox script will also finish and the timings displayed in respect to the intervals between triggers can also be saved.

In addition, the bpod protocol can be paused, restarted or stopped at any point. The pause instruction is handled at the beginning of a new trial and, when restarted or stopped, the settings,

events and time stamps from the interrupted session are saved, to still retain this information for possible analysis.

In summary, a session runs through sequenced trial matrices. Each of these is created in advance, simultaneously to the running of the preceding matrix. At each trial and state, bpod sends the appropriate triggers to the two photon system for image acquisition, and to the NIDAQ device, for stimulus presentation. In addition, bpod also sends triggers to the governing machine for parallel processing: updating the GUI displays, saving information and preparing the next matrix. Image 4.4 shows a simplified diagram of an example mini-session of 4 trials with the two-photon image acquisitions being started at every 2 trials.

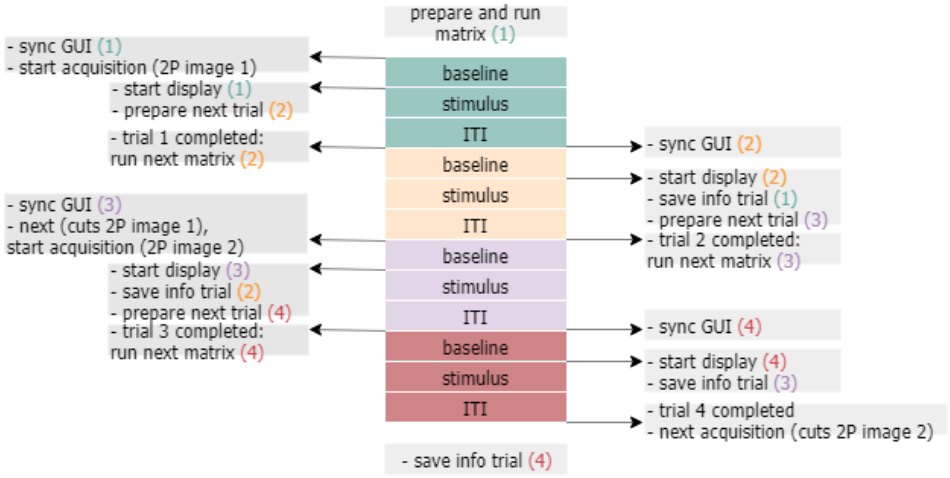

Figure 4.4: Diagram of the simplified states sequence in a session of 4 trials and two-photon acquisition triggers sent every two trials. The gray boxes indicate instructions, and the arrows represent the different trigger instructions sent at the state in its trailing edge. The colored parentesis refer to the trial that each instruction relates to.

5

Experimental Methods

Contents

Over the experimental process, the appropriate settings of both the animals' state of alertness and of the visual stimulation were chosen as an operative practical balance. In this chapter we describe the methods and specifications of the animals' care and craniotomy cirurgies, as well as the settings of the ISOI and visual stimulation sessions.

5.1 Animals

All procedures were approved by the Champalimaud Centre for the Unknown Ethics Committee and carried under the stipulations of the Portuguese Direção Geral de Veterinária. Mice were held in individual cages on a reversed light-dark cycle with access to food and water. Mice were exclusively used for the experiments regarding this thesis' work.

Cells' somata in V1 layer 2/3 of four Thy1-GCaMP6s ?? male?? mice (?? Laboratory stock no:??) were imaged.

Prior to the imaging experiments, once adults (?? to ?? weaks old), the mice underwent chronic window implantation surgeries. A circular craniotomy of diameter $4mm$ was performed over each mouse's left visual cortex, leaving the dura intact. The imaging windows were constructed using two layers of microscope cover glass (Fisher Scientific, no. 1 and no. 2) and UV-curable optical glue. A window was placed into the craniotomy using black dental cement and an iron headpost was attached to the skull with dental acrylic. The subjects were kept under isoflurane anesthesia, as well as Bupivacaine (0.05%; injected under the scalp) and Dolorex ($1mg/kg$; injected subcutaneously), serving respectively as local and general analgesia. Eye moisturing was insured with ophtalmic ointment (Clorocil, Laboratorio Edol).

For both the ISOI and visual stimuli protocols, the animals were lightly anesthetized with isoflurane (1%) and injected intramuscularly with chlorprothixene (1mg/kg), a muscular paralyzer to circumvert the need for higher anesthesia concentrations which could depress the recorded neuronal responses. Mice were headfixed by the headposts during all of the visual stimuli presentations and their eyes were protected and kept moist with silicone oil (Sigma-Aldrich) in thin, uniformly coated layers.

5.2 Visual stimulation

For both the ISOI and visual stimuli protocols, an LED display (BenQ XL2411Z, 144-Hz monitor, stimulus presented at $60Hz$) was used. The screen was placed at $15cm$ from the mouse's right eye and aligned at 30^o to the axis of its nose-line, insuring access to the visual space of 120^o in azimuth and 60^o in elevation???. The stimuli were produced and presented using Matlab and the Psychophysics Toolbox [REFERENCES] (chapter 3,??).

5.3 Intrinsic signal optical imaging settings

The course of action with each craniotomized mouse started with the performance of intrinsic signal optical imaging (ISOI) over the mice's primary visual cortex and surrounding visual areas [REFERENCES] to obtain a reasonable spatial resolution retinotopic mapping of the temporaly dependent

hemodynamics of the accessed brain while moving visual stimuli was presented to the animal on a monitor aligned to the center of the mouse's right eye and forming a 30º angle with the animal's nose-line.

The stimuli consisted of a checkerboard of alternate flickering light/dark squares ($5Hz$) that was masked to continuously expose only a periodic drifting stripe of the grid in four consecutive cardinal directions ($12s$ period, 20º width, 80 times for each direction) - an horizontal stripe going from the top to the bottom of the screen, vice-versa, a vertical stripe going from its left to its right or in the opposite direction.[GET IMAGE]

The cortical surface of an head-fixed mouse was illuminated with a $620nm$ red LED to allow the intrinsic hemodynamic signals to be recorded as optical images of reflectance change correspondent to cortical activity. This recording was held using a Retiga QIClick camera (QImaging) controlled with Ephus[REFERENCE] with a high magnification zoom lens (Thorlabs) at $5Hz$ focused under the cranial window, at the brain surface. A $535nm$ green LED was also used to obtain an image of the cortical vasculature.

For each animal, this resulted in a retinotopical map of 512×512 pixels, representing ??×?? of cortical area. This corresponded to the color-map of cortical encoding of both azimuth and elevation stimuli locations, superimposed on the image of the mouse's vasculature[GET IMAGE]. These correspondence figures were subsequently used as a first-approach guide to encountering the V1 positions aimed for imaging - those whose neurons responded to stimuli in the center of the mouse's visual field where the central stimuli were displayed during the following two-photon microscopy imaging sessions.

5.4 Session and trial structure

5.4.1 TPLSM experimental pipeline

An imaging session followed the same process in each experiment, starting with the setting up of a rig. As a first step, the laser was turned on from its standby mode, about 30 minutes before conducting the scanning. This was the required time for the device to warm up to consistent power levels.

Besides the laser, the objective's motor, connected to the two-photon computer, was also turned on, as well as the heating pad to place the animal on and keep its thermal balance whilst anesthetized. The laser's shutter was also opened as well as the pockel cells that control the light delivered to the animal's brain. Furthermore, the laser source was shared between two rigs, which meant that at each session one should confirm that the mirrors were rotated to the appropriate angle to send light to the rig being used. Furthermore, the system had two operation modes that could be interchanged with a switcher: Full brightness and two-photon imaging modes. With the PMT off, the experiment was to start with the switch to full brightness mode.

During this time, both the stimuli computer and the two-photon computer were turned on, and the rig was wired to bpod mode. In the stimuli computer, two matlab instances were open, one for bpod states machine and GUI and another for psychtoolbox's stimuli presentation. In the two-photon computer, Bonsai light contamination control system was put to play, and a matlab instance was opened to start scanImage 4 laser-scanning software control system.

The animal to be imaged was manually removed from its cage and placed in a box to be anesthetized with isoflurane, initially at 3.5%, delivered by a ventilation tube, mixed with oxygen at pressure of $1atm$. Once the animal was unconscious, the paralyser chlorprothixene ($1mg/kg$) was injected intramuscularly, and the animal was put back in the anaesthetizing box. At this point, the isoflurane ventilation was switched from the box to the rig's tube and the animal was quickly and carefully moved from the box to a platform in the rig under the objective, over the heating pad, confirmed to be at $34°C$, with a mouth piece connected to the anaesthesia tube surrounding its fur. The mouse's headpiece was then locked to fixation screws and the animal's eyes were protected with an uniform layer of eye ointment and the anaesthesia was set to a 1% value, to maintain during the rest of the session.

The cranial window was cleaned with deionized water as well as the objective, with the aid of Thorlab paper for optical components. A black plastic ring was then glued to the cranial window, in order to minimize contamination of the signal with monitor light. Imaging gel was placed over the cranial window, with care for not keeping air bubbles that could impeach the light path, and for keeping full uniform contact between the gel and the imaging window.

The imaging system was initially in full brightness mode with the PMT turned off. ??? software was then opened and configured in the two-photon computer, to aid with full-brightness mode navigation. With this, a pedal allowed a green light to be sent from the objective, aiding in the alignment of the animal's cranial window within the full range of the objective's motor: the animal's platform was moved to the appropriate objective-aligned placing and the objective was then moved down in depth until reaching the gel and until the software displayed visible blood vessels [IMAGE]. The stimuli presentation monitor was then centered to the animal's right eye gaze, at $15cm$ from his eye and at a $30°$ angle with its body's axis. Finally, a light shield was placed over the objective and the rubber ring in the animal's cranial window, ensuring good blockage of the monitor's contamination light to the signal's light path. The room's lights were filtered for only passing red light and the rig was then closed with a black cloth to further seclude it from light contamination and PMT damage.

With the intrinsic azimuth and elevation maps rotated to match the objective's signal display on SOFTWARE with the green light on, one would then search for the (0,0) corresponding position in V1, using the larger blood vessels as guidelines. Having found this placing, the pedal was left off, and the PMT could be turned on for two-photon mode imaging with the scanImage software.

The configurations in ScanImage were set to multiplane scanning (5 planes) and the further settings in table ???. The laser was calibrated, and the voltage - angle calibration curve is to have the shape in [IMAGE]. Bpod was started with a Tuning protocol, with a small-sized circular center grating stimuli being presented in multiple directions and frequencies, to further aid in searching for V1 (0,0) position. The bpod setting's were submitted, and the psychtoolbox protocol could be initiated, preparing the stimuli.

The scanning could be started with the "Grab" button in ScanImage GUI and no external triggering, for continuous signal collection through time. The experimenter can then see the green channel's signal for each imaged plane, in the ScanImage GUI. Going down in depth, one starts to detect the

dura of the brain. At this point, the motor coordinates should be set to zero. I then went further down to $150\mu m$ to $210\mu m$ center plane depth, until neurons could be detected [IMAGE].

Once the stimuli masks were ready, the "Start" button in bpod's GUI initiated the stimuli presentation. With this small centered stimuli being displayed to the mouse, I could then search for the close positions in the mouse's brain that were more strongly responding with locked timings to the stimuli presentation.

Having found this position, the recordings were started, fixed to external triggering from bpod. A reference image was print screened and kept for checking and managing possible drift of the imaging planes during the session, due to cranial window or brain micro movements. During the session, the experimenter should also keep checking the trial number synchronization between scan image recordings, psychtoolbox presentation and bpod triggers.

5.4.2 Stimuli presentation structure

The experimental recorded stimuli presentation of a session comprised three main protocols for each mouse and each of that animal's V1 imaged position: A protocol to establish the receptive fields of the imaged neurons (`StimPresProt_RF`), another to regard their tuning properties (`StimPresProt_tuning`) and a last protocol designed for the actual surround modulation examinations (`StimPresProt_RF`).

Each protocol involved a pseudorandomized sequence of trials - N repetitions of X trial types. Repetitions of each stimulus type are required in order to enhance the signal to noise ratio of the responses by trial averaging.

In general, each trial was formed by an initial baseline, a stimulus presentation, and an inter-trial interval (ITI). In both the baseline and the ITI the screen was left at background brightness and contrast level (grey) and its duration was used as buffer time for internal computations and to ensure sufficient Calcium decay from the previous stimulation (from the previous trial in the case of the baseline, and from the same trial in the case of the ITI). A session's total stimuli display duration should not be longer than two hours, as the anesthesia produces cumulative effects in the central nervous system and can start depressing the neuronal responses, impeaching the subsequent study of its relation with the visual stimulation [REFERENCES]. Thus, the durations of these intervals depended on the specific protocol (chapter 4, section d), as a balance between how important was the separation of responses in between trials - the more precise the intended separation, the larger should be the baseline and ITI durations - and how many trial types and trial repetitions were intended - the more trials, the less duration the baseline and ITI should have.

	Number of trial types	Number of repetitions	baseline (ms)	stimulus (ms)	ITI (ms)
RF	80	14	0	880	120
tuning	32	25	5	900	95
SM	124	15-20	500	1000	500

Table 5.1: Protocol configurations regarding session extension and trial durations.

5.5 Specifics of the protocol settings and visual stimuli

In a session, the three stimuli presentation protocols were ordered as RF mapping, tuning mapping and then the actual SM examination. Each protocol is associated with different stimuli characteristics, specific to the controls or information that were to be required from the final extracted data. Furthermore, each kind of protocol had also distinct specifications in regards to the time durations in the trial structure of the session. The mice were always placed with their right eye parallel and at $15cm$ from the center of the monitor. All of the stimuli measurements will thus follow indicated in degrees at the mice's perspective to the screen, in azimuth (horizontal axis) and in elevation (vertical axis) coordinates. In addition, to compensate for the screen's flatness, spherical corrections were applied to the displayed stimuli, so that what the mice visualized corresponded to the same size of stimuli at each patch location, irrespective of its distance in the screen and that no distortions in the gratings were perceived by the animal. Every protocol underwent pseudorandomization of the trials: Each type of trial appeared the same number of N repetitions, but at shuffled order. The reason for this was to minimize the neurons adaptation [REFERENCES] to the specific trial types, as they had to be repeated a reasonable amount of times for significant analysis.

5.5.1 Receptive Field mapping stimuli

This protocol consisted on the presentation of a 10^o squared cell (in the mouse's referential) with a small moving bar inside. At each trial, this bar moved in four directions, in sequence but at random order - bottom to top (labelled 0^o), left to right (90^o) and the opposite ones (180^o and 270^o, respectively). The moving bar had 4^o width and $25^o/s$ speed, with the dark at $0WHAT$, the light at $204WHAT$ and the background at $102WHAT$. This patch appeared in any of 80 positions in the monitor, which was divided in a 10×10 grid, tiling a circle with 50^o maximum radius from the center. The presentation was repeated in each grid position 14 times, to a total of 1120 trials, at shuffled order whithin each repetition.

At each trial of $1s$, the stimulus played for $220ms$ and was followed by an $880ms$ ITI, summing 19 minutes of RF mapping at each session.

[GET IMAGE]

Feature	Value
cell size (^{o})	10
cell grid (^{o})	[10, 10]
maximum radius (^{o})	50
stim directions (^{o})	[0 90 180 270]
bar width (^{o})	4
bar speed (^{o}/s)	10
dark, stim, background light	[0 204 102]

Table 5.2: Configurations regarding the RF mapping protocol stimuli properties.

5.5.2 Tunings mapping stimuli

The selectivity of each neuron was also controlled for spatial and temporal frequencies, as well as for more gratings' directions of movement.

With the same contrast configurations as for the previous protocol, a circular centered patch of 30º was presented at any of 8 directions: the previous and the intermediatedly oriented ones (0º, 45º, 90º, 135º, 180º, 225º, 270º and 315º). The gratings could have 0.02/º or 0.04/º of spatial frequency and $0.5Hz$ or $1Hz$ as temporal frequency. Together, each of these 32 configurations of direction and frequencies were presented in 25 repetitions, totaled at 800 trials and shuffled within the full protocol.

Each trial had $1s$, divided in a baseline of $5ms$, a stimulus presentation of $900ms$ and an ITI of $95ms$, to a total of 14 minutes per session.

Feature	Value
stimulus size (º)	30
stimulus center (º)	[0, 0]
stim directions (º)	[0 45 90 135 180 225 270 315]
spatial frequency (/º)	[0.02 0.04]
temporal frequency (Hz)	[0.5 1]
dark, stim, background light	[0 204 102]

Table 5.3: Configurations regarding the tuning mapping protocol stimuli properties.

5.5.3 Surround Modulation stimuli

Finally, for the SM protocol the frequencies of 0.04/º and $1s$ were chosen based on previous reports of largest V1 stimulation [REFERENCES]. The light contrasts of the gratings went from 0 at dark to 122.5 at background and 255 at the lightest. Each trial had $2s$, with $0.5s$ of baseline, $1s$ of stimuli display and $0.5s$ of ITI.

There were 124 possible trial types, repeated 20 times, to a total of 2480 trials in an 1 hour and 23 minutes session.

Feature	Value
spatial frequency (/º)	0.04
temporal frequency (Hz)	1
central radius (º)	15
surround inner and outer radius (º)	[27 50]
stim directions (º)	[0 90 180 270]
dark, stim, background light	[0 255 122.5]
groups of stimuli	C, S1, S1+C, S2, S2+C

Table 5.4: Configurations regarding the SM protocol stimuli properties.

There were 5 possible patches: a central one and four surround patches in the cardinal positions. The central patch was a circle of 15º radius, as the others were limited by an external circumference of 50º, an inner circumference of 27º (to obtain a 12º gap between the center and the surround patches) and the curresponding bissectors of the screen. For any patch, there were 4 available directions of gratings movement (0º, 90º, 180º and 270º).

With these patches, five groups of stimuli types were used:

- C - only the center patch, in any of the 4 directions of movement (4 types);
- $S1$ - only one surround patch, in any of the 4 cardinal top, bottom, left or right locations (S1T, S1B, S1L, S1R), and in any of the 4 directions (16 types);
- $S1 + C$ - One surround patch and the center patch, at any location of the surround($S1T + C$, $S1B + C$, $S1L + C$, $S1R + C$) and any direction for the center and for the surround (64 types);

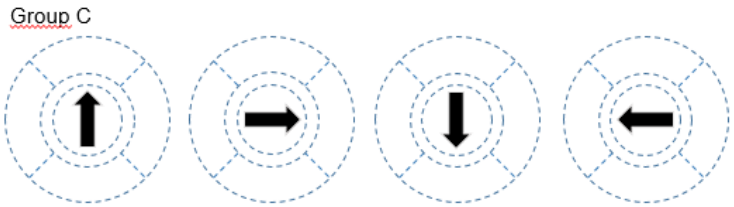

Figure 5.1: Diagram of stimuli group C.

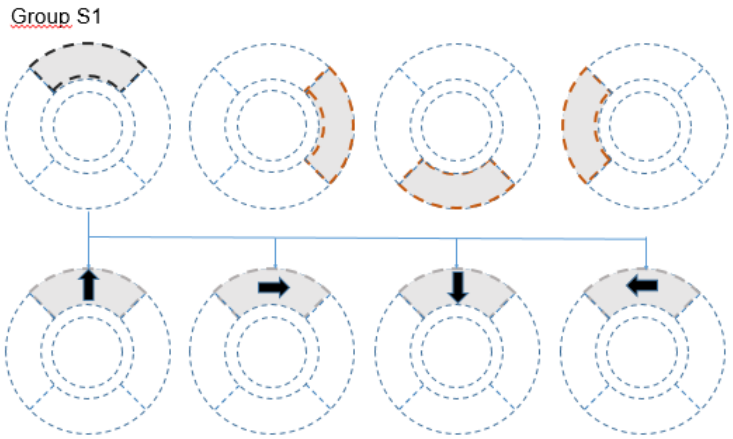

Figure 5.2: Diagram of stimuli group S1.

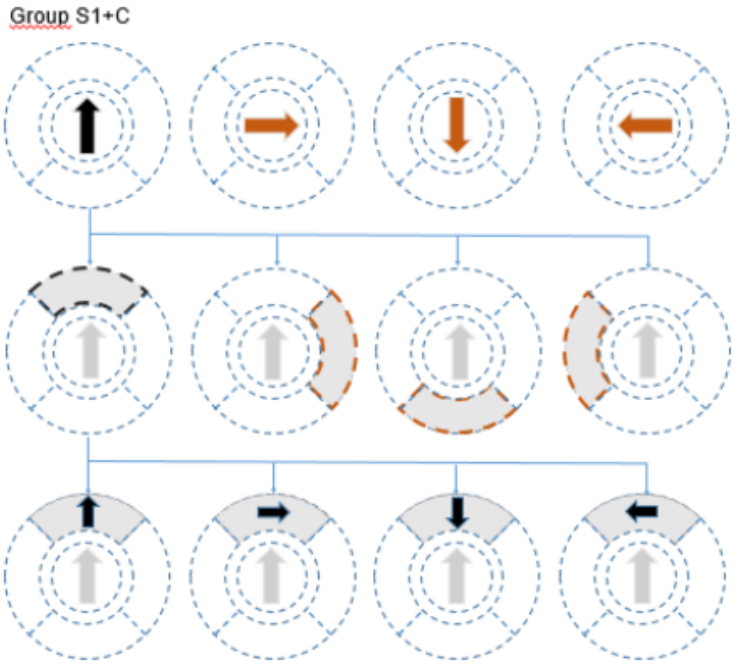

Figure 5.3: Diagram of stimuli group S1C.

- $S2$ - only two surround patches, in opposite cardinal locations, either in the horizontal line ($S2H$) or the vertical line ($S2V$), both of them with gratings moving in the same of any of the 4 directions (8 types);

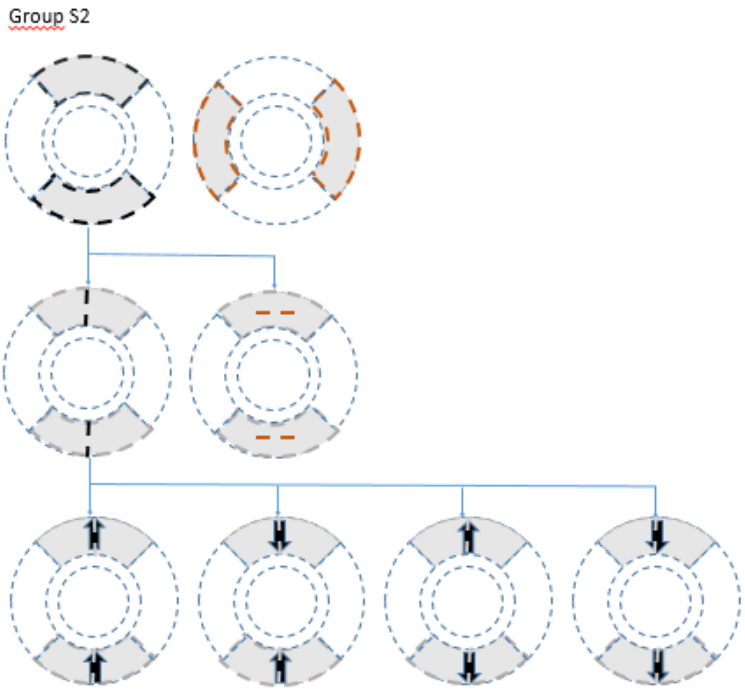

Figure 5.4: Diagram of stimuli group S2.

- $S2 + C$ - Two surround patches and the center patch, both surround patches either in the horizontal ($S2H + C$) or the vertical line ($S2V + C$), both with gratings moving in the same of the possible directions and the center patch with gratings moving in any direction, not necessarily being the same from the surround stimuli (32 types).

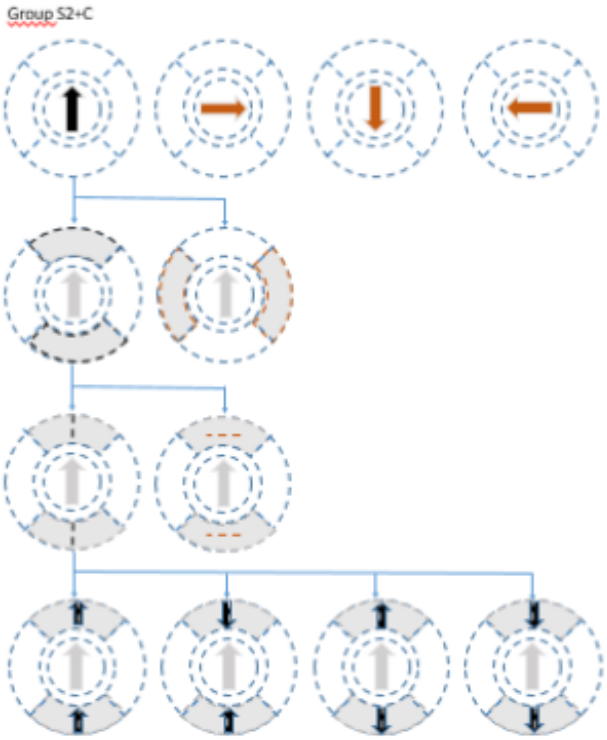

Figure 5.5: Diagram of stimuli group S2C.

Group C was used as a more specific confirmation for the receptive field findings: here the stimuli was now in the center of the screen with the selected size for the analysis. Groups $S1$ and $S2$ provided the data that allowed to exclude from the analysis the cells that responded to stimulation in the defined surround. These had a receptive field that overlapped what we regarded as the surround and thus did not meet the criteria for investigating surround modulation effects in this experiment's designed manner. With the cells that did respond to group C but did not to group $S1$ nor $S2$, we could then regard the effects of actual surround stimulation by examinating the responses to stimuli in the groups $S1 + C$ and $S2 + C$.

6

Analysis

Contents

Upon the experimental procedures, a developed pipeline was followed for the analysis of the RF, tuning and SM protocols, for each animal and imaging session. This process will be described hereby, along with the explanation of each utilized tool, analysis scripts and software. In particular, for this project's experiments' analysis, Suit2p software for automated selection of neurons in a raw image and corresponding fluorescence traces extraction was implemented. This package will here be presented and compared with previously used methods.

6.1 Experiment's outputs

Once an experiment is completed, a set of raw images, the corresponding stimuli information and event timings will be available. Corresponding to a protocol, there will be a set of frames for each trial, according to the TPLSM system's scanning speed of $30Hz$ and the 5 planes being processed ($6Hz$ per plane). For instance, the RF protocol comprises 1120 trials and the triggers sent from bpod to the imaging computer for dividing the images come at each 4 trials. There are thus, for this case, 280 sets of images. Since each trial endures for $1s$, each of these sets contains 6 frames for each of the 4 relevant planes, prefacing, for the RF protocol, 24 total frames per trial. In turn, each of these frames contains a 512×512 pixels image of the fluorescent signals emitted from the animal's brain and detected at that time[IMAGE-WHAT DO THE PIXELS CORRESPOND TO IN SIZE]. For each of the trial's sets of images, there is the corresponding stimulus information being saved in a Matlab structure: In the case of the RF, the changing feature is the position of the stimulus patch being presented in the screen during that trial, for the Tuning protocol these are the spacial and temporal frequencies as well as the direction of the centred stimulus, and finally for the SM protocol the independent variable is the stimulus type number. Apart from these, also the constant features of the stimuli at each protocol are saved in the same structure. The trial time stamps in bpod's triggering, states and Psychtoolbox's clocked timings from a received trigger to the next are also saved. This allows, in the latter analysis, to confirm and if need correcting the stimulus information in the case of any eventual skipped trials. Finally, Scan Image configurations are also saved, in each trial's video header, keeping the information required about the laser's power during that experiment, multiplane settings and read offsets.

6.2 Images pre-processing: Separating planes and registration

6.3 Suit2p pipeline

The recordings from two-photon microscopy and calcium indicators yield the observation of large neuron populations' activity that must be processed in a suitable way to extract neuron's fluorescence traces. This data comprises multi-plane movies of a great number of cells, depending on the imaged region. Computational methods for its treatment should be not only accurate, but fast, as to grant the feasibility of substantial data's processing.

In this project, the *Suite2p* pipeline will be used. This set of algorithms implements four modular processing independent steps: Image registration from raw movies through phase correlation, the detection of regions of interest (ROIs), their interactive labelling and quality control and finally the

extraction of a single representative fluorescence signal for each ROI.

The first stage is image registration, spatially aligning images taken at different times or from different viewpoints. The algorithm receives raw movies as inputs and corrects for the effects of brain movement.

The second stage uses the aligned movies and selects spatial regions of interest (ROIs) - somata, dendrites, spines or butons - with each pixel assigned to a positive weight. The model assumes the origin of the recorded signal in each pixel to be coming from three possible origins: the actual ROIs, measurement noise, but also from the neuropil - synaptically dense regions, out-of-focus dendrites and axons whose average activity contaminates the detection with a large and diffuse signal.

The third stage amounts to the quality control of the classification, distinguishing between cell and non-cell (compartments, such as dendrites or axons), and lowering the fluorescence variance in each ROI. This is firstly done by an automated classifier and then curated by the used through the software's GUI that displays an improved resolution image, each ROIs information, and allows its relabelling as cell/non-cell.

Finally, the fourth stage of the pipeline outputs, for each ROI, a single calcium fluorescence time-varying signal. Again, this signal is corrected for the neuropil contamination signals. Furthermore, the spike train - the action potential sequence - that causes this signal is estimated, by use of a fitting model.

This processed data will be the substance for the posterior statistical study that will finally allow the aimed understanding of structural principles for surround modulation with moving stimuli in all the underwent experimental configurations of parameters and the consequent possible postulation of further V1 surround modulation rules.

6.3.1 Registration

6.3.2 Selection of regions of interest (ROIs)

6.3.3 ROI labelling and quality control

6.3.4 Trace extraction and spike deconvolution

6.4 Data treatement

6.4.1 Receptive field mapping

6.4.2 Tuning mapping

6.4.3 Surround modulation protocol

7

Results

Present the chapter content.

8

Conclusions and Future Work

Conclusions Chapter

A

Title of AppendixA